Organic Geochemistry 121 (2018) 138–154

Contents lists available at ScienceDirect

Organic Geochemistry

journal homepage: www.elsevier.com/locate/orggeochem

Change in provenance of branched glycerol dialkyl glycerol tetraethers over the Holocene in the Baltic Sea and its impact on continental climate reconstruction

Lisa Warden [a,1], Matthias Moros [b], Yuki Weber [c,2], Jaap S. Sinninghe Damsté [a,d,*]

[a] NIOZ Netherlands Institute for Sea Research, Department of Marine Microbiology and Biogeochemistry, and Utrecht University, PO Box 59, 1790 AB Den Burg, Netherlands
[b] The Leibniz Institute for Baltic Sea Research, Department of Marine Geology, Seestraße 15, D-18119 Rostock, Warnemünde, Germany
[c] University of Basel, Department of Environmental Sciences, Bernoullistrasse 30, 4056 Basel, Switzerland
[d] Utrecht University, Faculty of Geosciences, Department of Earth Sciences, P.O. Box 80.021, 3508 TA Utrecht, The Netherlands

ARTICLE INFO

Article history:
Received 7 December 2017
Received in revised form 28 February 2018
Accepted 18 March 2018
Available online 12 April 2018

Keywords:
Baltic Sea
Branched vs. isoprenoid tetraether (BIT) index
Branched GDGTs
Isoprenoids GDGTs
Holocene
Temperature reconstruction
Lake
Coastal sea

ABSTRACT

The Baltic Sea is an enclosed basin that experienced a number of different salinity phases during the Holocene corresponding to the establishment of a connection with the North Sea. Branched glycerol dialkyl glycerol tetraethers (brGDGTs) in surface sediments and Holocene sedimentary successions from the Gotland and Arkona Basins were analyzed to examine their potential applicability as indicators for soil organic matter input, as well as their suitability for paleoclimate reconstructions. Our results show a marked change in brGDGT distributions and the branched and isoprenoid tetraether (BIT) index. The transition of the Ancylus Lake (fresh) to the Littorina Sea (brackish) phase is revealed by a large drop in the BIT index and an increase in the MBT'_{5Me}, which reveals a large shift in provenance of the sedimentary brGDGTs. During the lake phase, brGDGTs are presumed to be primarily produced by in situ production in the water column. During the brackish phase, in situ brGDGT production in the alkaline pore waters of the surface sediments (as revealed by their high degree of cyclization) was predominant although there was evidence of occasional input of soil-derived brGDGTs. The predominant aquatic autochthonous production of brGDGTs does not allow the use of brGDGTs for continental air temperature reconstructions but they can be used for bottom water and lake temperature reconstructions during some intervals. The results from this study demonstrate that geological changes and concomittant salinity variations can be revealed by the provenance of brGDGTs.

1. Introduction

Investigating climatic variability is important for predicting future climate change as well as how ecosystems, organisms and human society could be affected. To better understand past climate systems, more reliable continental climate data are necessary and so is further research on developing and improving terrestrial climate proxies. Branched glycerol dialkyl glycerol tetraethers (brGDGTs; see Fig. 1 for structures) are biosynthesized by bacteria (Weijers et al., 2006a) and their occurrence was initially thought to be restricted to soils and peats (Hopmans et al., 2004; Weijers et al., 2006b). Their distribution, expressed by the degree of methylation (methylation index of branched tetraethers; MBT) and cyclization (cyclization index of branched tetraethers; CBT), has been shown to correlate with soil pH and mean annual air temperature (MAT) (Weijers et al., 2007a). The preserved distribution of these fossilized membrane lipids has been used for paleoclimate reconstructions in coastal marine sediments (e.g. Weijers et al., 2007b; Bendle et al., 2010), paleosoils (e.g. Peterse et al., 2011; Zech et al., 2012), peats and coals (e.g. Weijers et al., 2011; Naafs et al., 2017), and lacustrine sediments (e.g. Zink et al., 2010; Loomis et al., 2012; Niemann et al., 2012). In marine and lacustrine sediments the bacterial brGDGTs were initially assumed to originate predominantly from continental soil erosion and terrestrial runoff, whereas the isoprenoid GDGTs (isoGDGTs; including crenarchaeol, the GDGT specific to Thaumarchaeota; Sinninghe Damsté et al., 2002) were thought to be mainly produced by aquatic ammonia-oxidizing archaea. Capitalizing on their terrigenous

* Corresponding author at: NIOZ Netherlands Institute for Sea Research, Department of Marine Microbiology and Biogeochemistry, and Utrecht University, PO Box 59, 1790 AB Den Burg, Netherlands.
E-mail address: J.S.SinninghеDamste@uu.nl (J.S. Sinninghe Damsté).
[1] Current address: Carnegie Institute for Science, Geophysical Laboratory, Washington, D.C., USA.
[2] Current address: Harvard University, Department of Earth and Planetary Sciences, Cambridge, MA 02138, USA.

https://doi.org/10.1016/j.orggeochem.2018.03.007
0146-6380/

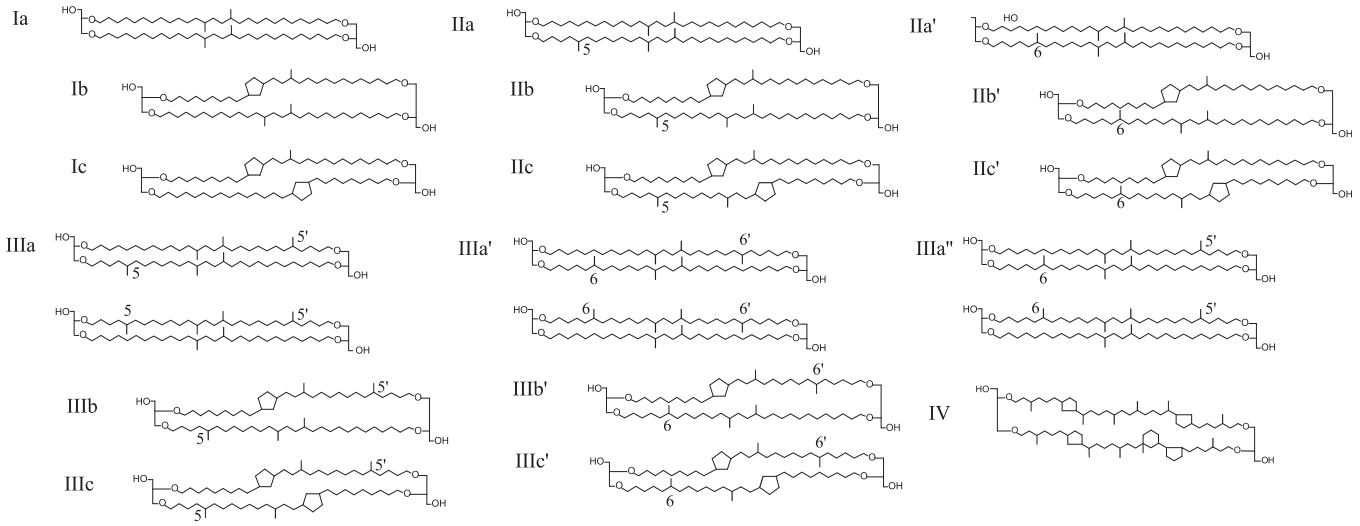

Fig. 1. Chemical structures of the widespread brGDGTs (I-III; Sinninghe Damsté et al., 2000; Weijers et al., 2006a; De Jonge et al., 2013), the novel brGDGT isomer IIIa″ (Weber et al., 2015), and crenarchaeol IV (Sinninghe Damsté et al., 2002). The molecules designated with a prime symbol are referred to as the 6-methyl brGDGTs.

origins, the branched vs. isoprenoid tetraether (BIT) index was developed, representing the ratio of the major brGDGTs over crenarchaeol, as a proxy for terrestrial organic matter input into a region (Hopmans et al., 2004). Complications using brGDGTs for climate reconstructions have arisen in areas with low terrestrial input as determined using the BIT index (Peterse et al., 2009; Zhu et al., 2011). In situ production of brGDGTs in aquatic environments has also been shown to alter their distribution and thus affects the use of these proxies (Peterse et al., 2009; Zhu et al., 2011; Loomis et al., 2011; Zell et al., 2013; Buckles et al., 2014; Sinninghe Damsté, 2016) and so it is recommended to understand the provenance of brGDGTs in a region before attempting paleoclimate reconstructions (Zell et al., 2013; De Jonge et al., 2015a).

To date, most brGDGT-based paleoclimate reconstructions are based on a suite of nine components with six of them containing a 5-methyl substituent (Fig. 1). However, in addition to these 5-methyl brGDGTs, six novel 6-methyl brGDGTs were recently discovered and shown to be co-eluting with the 5-methyl brGDGTs employing the commonly used separation methods (De Jonge et al., 2013). In lake sediments, 7-methyl brGDGTs have been shown to comprise up to 6% of the total brGDGTs (Ding et al., 2016). Using improved chromatography methods (Hopmans et al., 2016), the separation and quantification of 5- and 6-methyl brGDGTs has led to the definition of new indices (De Jonge et al., 2014a, 2014b) and the improved MAT reconstructions based on a global soil calibration (De Jonge et al., 2014a), a global peat calibration (Naafs et al., 2017), and an African lake calibration (Russell et al., 2018).

The Baltic Sea (BS) is a large, brackish body of water with a high terrestrial influence, which makes it an interesting region for examining if sedimentary brGDGT records can be used for climate reconstruction. In this study, we examine Holocene sedimentary sections, covering varying phases, from two locations in the BS proper, as well as eleven surface sediments from around the BS and two from the Skagerrak. Through examination of concentrations and distributions of iso- and brGDGTs, and BIT index values, we gain further insight into how GDGT distributions were affected by the physical and chemical changes that took place during the Holocene (see Section 2). By making comparisons to present day conditions we gain understanding about how such changes may affect brGDGT-based paleotemperature reconstructions, as well as whether these lipids can be indicators of other environmental changes.

2. Study site

The BS (Fig. 2) has an area of about 377,000 km^2 that is broken up into multiple sub-basins. It receives 660 km^3 of freshwater (including precipitation) per year from a drainage basin that has an area of 1.6 million km^2 (Björck, 1995). Substantial amounts of saline water (475 km^3/yr) flow from the only connection to the North Sea through the narrow Straits of Denmark (Tikkanen and Oksanen, 2002). The total outflow of brackish water is ca. 950 km^3/yr (Björck, 1995). Although the BS is the world's largest brackish body of water, it is fairly shallow and on average is only 54 m deep (Emeis et al., 2003). Its salinity varies greatly ranging from ~3.5 in the north to ~8 in the central BS and ~30 in the Skagerrak, the region where the BS connects to the North Sea. A salinity gradient also exists between the surface and deep waters, separated by a permanent halocline at about 30 m depth. The air temperatures around the basin range from almost 0 °C in the winter to more than 20 °C in the summer (Wasmund, 1997). Presently the BS is persistently stratified resulting in anoxic bottom waters in the deeper basins as well as hypoxic coastal areas.

The BS has gone through several phases since the last deglaciation; the Baltic Ice Lake, the Yoldia Sea, the Ancylus Lake, the Littorina Sea and the modern BS. The Baltic Ice Lake was created ca. 14,000 BP by a retreating ice sheet that blocked water exchange with the North Sea (Björck, 1995). After the ice sheet retreated, the connection to the ocean was opened and an influx of marine water created the slightly brackish conditions of the Yoldia Sea (Jensen, 1995; Björck et al., 1996). The following post-glacial rebound and uplift of land once again restricted the connection between the basin and the ocean (Jensen et al., 1999), resulting in the freshwater Ancylus Lake (Björck, 1995). Eustatic sea-level rise initiated a reconnection to the ocean allowing the inflow of salt water and transforming the lake into the Littorina Sea (Winterhalter, 1992). The Ancylus Lake/Littorina Sea transition is considered to be very complex and consisted of weak pulses of higher salinity waters entering the basin for almost 2000 years before fully brackish conditions were established (Andrén et al., 2000a). The Littorina Sea is considered to have had the most marine-like conditions of the BS since the deglaciation (Andrén et al., 2000b), while the present day BS is regarded as a continuation of this phase with lower salinity (Punning et al., 1988). The higher summer see surface temperatures (SSTs) starting at around 6.0 cal kyr BP in the BS are believed to have initiated the onset of anoxia in regions of the

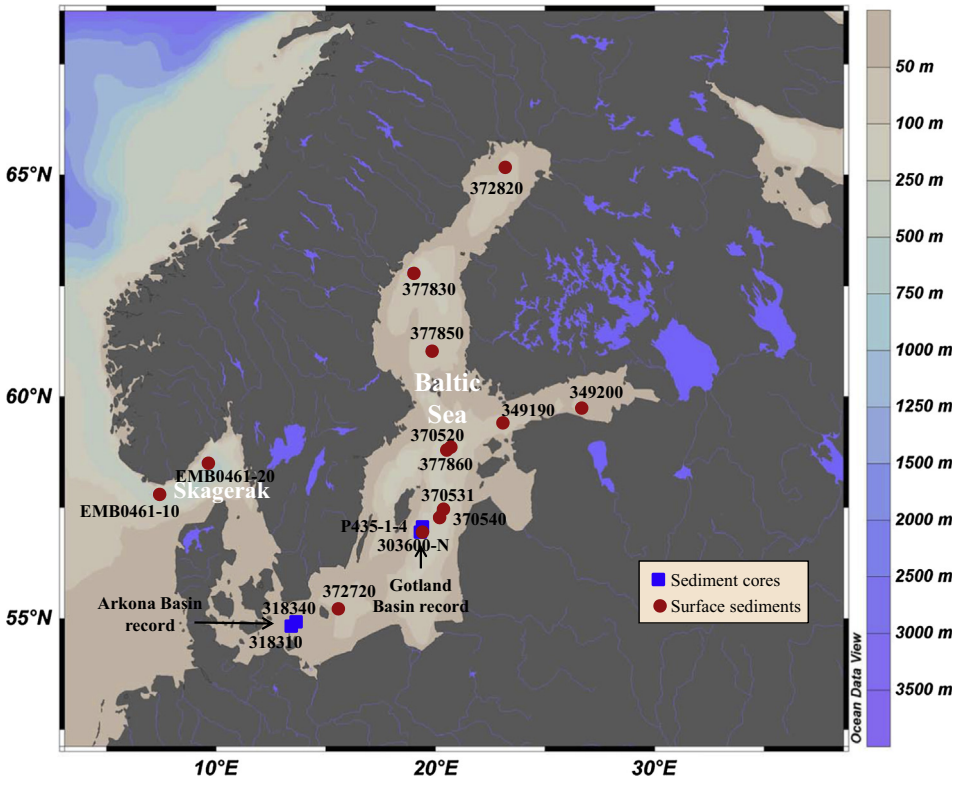

Fig. 2. The location of the study sites. Surface sediments were collected form eleven locations, indicated by red circles, in the BS and the Skagerak. Sediment cores were obtained from four locations, indicated by blue squares, in the Gotland and Arkona basins. (For interpretation of the references to color in this figure legend, the reader is referred to the web version of this article.)

basin (Warden et al., 2017). When summer SSTs subsequently decreased by 1–3 °C during the post Littorina Sea phase (starting ca. 4.3 cal kyr BP) anoxic conditions were not reestablished in the BS for a period of about 3000 years until a subsequent increase in summer SST at around 1.4 cal kyr BP (Warden et al., 2017).

3. Experimental methods

3.1. Sampling

Eleven surface (0–1 cm) sediments from the entire BS basin (Fig. 2) were used. Their sampling is described in Kabel et al. (2012). Two Skagerrak surface (0.0–0.5 cm) sediments (Table 1; Fig. 2) were collected using a multi corer during cruise EMB046 of the R/V *Elisabeth Mann-Borgese* in May 2013.

Four sediment cores from two locations (Table 1; Fig. 2) were studied. A multicore (MUC P435-1-4) from the Gotland Basin was collected during the R/V *Poseidon* cruise P435 in June 2012. A gravity core (GC 303600-N) was collected at the same location during a R/V *Prof. Albrecht Penck* cruise in July 2007. This core (0–377 cm) covers the brackish, the Ancylus Lake, and part of the Yoldia Sea phase (Sollai et al., 2017). An age model for the 80–210 cm of this core has been previously established using radiocarbon dates of benthic foraminifera (Warden et al., 2017). Sediment core P435-1-4 MUC (0–52 cm) contains the most recent sediments and partially overlaps with core GC 303600-N, based on the TOC profiles (Sollai et al., 2017). Samples were plotted on a composite depth scale by adding 34 cm to the depth of the samples of the GC 303600-N core.

Two gravity cores were collected from the Arkona Basin on a cruise of the R/V *Maria S. Merian* in April 2006. For these cores (318340, 0–670 cm, and 318310, 0–1160 cm) an age-depth model is available (Warden et al., 2016a) and the combined record covers the last part of the Baltic Ice Lake period, the Yoldia Sea phase, the Ancylus Lake stage, and the Littorina Sea (or brackish) phase. The data were plotted on a composite depth scale by converting the expanded depth scale of core 318340 to that of core 318310.

3.2. Lipid extraction and GDGT analysis

All sediment samples were freeze-dried, and then after being ground and homogenized using a mortar and pestle, extracted using the Dionex™ accelerated solvent extraction (ASE). Sediments (1–3 g) were extracted with a solvent mixture of dichloromethane (DCM):methanol (9:1, v/v) at a temperature of 100 °C and a pressure of 1500 psi (5 min each). The collected extract was concentrated with a Caliper Turbovap®LV, and dried over anhydrous Na_2SO_4 and blown down over a gentle stream of N_2. In order to quantify GDGTs, 1 μg of an internal standard (C_{46} GDGT; Huguet et al., 2006) was added to the total lipid extract before separating it over an Al_2O_3 column (activated for 2 h at 150 °C) into three fractions using hexane:DCM (9:1, v:v) for the apolar fraction, hexane:DCM (1:1, v:v) for the ketone fraction, and DCM:MeOH (1:1, v:v) for the polar fraction. The polar fraction containing the GDGTs was dried under N_2 and then re-dissolved in hexane:isopropanol (99:1, v:v) at a concentration 10 mg ml^{-1} before being passed through a 0.45 μm PTFE filter and analyzed with ultra high performance liquid chromatography-atmospheric pressure positive ion chemical ionization–mass spectrometry (UHPLC-APCI-MS) using the method described by Hopmans et al. (2016). Selected ion monitoring of specific ions was used to quantify crenarchaeol and the brGDGTs; for a selected set of samples GDGT-0 was also quantified using a second run. The concentration of brGDGTs were normalized on the total organic carbon (TOC) content. TOC data for cores P435-1-4 MUC and GC 303600-N have been published previously (Sollai et al., 2017). For the Arkona cores only loss in ignition

Table 1
Location and water depths of surface sediments and sediment cores used in this study and MAT data of nearby weather stations where appropriate.

Station	Location	Latitude [N]	Longitude [E]	Water depth [m]	MAT[b] (°C)
Surface sediments					
372820[a]	Bothnian Bay	65°10.70	23°05.73	122	1.4
377830[a]	Bothnian Sea	62°50.71	18°53.34	210	4.1
377850[a]	Bothnian Sea	61°04.31	19°43.68	136	4.5
349190[a]	Gulf of Finland	59°26.09	22°58.39	94	6.9
349200[a]	Gulf of Finland	59°46.97	26°35.05	82	6.9
370520[a]	Central Baltic	58°53.66	20°34.43	182	6.9
377860[a]	Central Baltic	58°48.92	20°25.17	195	6.9
370531[a]	Gotland Sea	57°23.12	20°15.55	232	7.2
370540[a]	Gotland Sea	57°17.04	20°07.26	243	7.2
303600[a]	Gotland Sea	56°55.01	19°19.99	170	7.2
372720[a]	Bornholm Sea	55°15.67	15°28.21	96	8.1
EMB046-10	Skagerrak	57°49.74	07°17.66	457	n.a.
EMB046-20	Skagerrak	58°31.60	09°29.09	532	n.a.
Cores					
303600-N	Gotland Basin	56°55.01	19°19.99	170	n.a.
P435-1-4	Gotland Basin	56°57.94	19°22.21	178	n.a.
318310	Arkona Basin	54°50.34	13°32.03	46	n.a.
318340	Arkona Basin	54°54.77	13°41.44	47	n.a.

[a] These sediments were collected previously (Kabel et al., 2012).
[b] MAT (°C) values are from the closest weather station (www.rimfrost.no) and an average over the period of 1890–2016.

(LOI) data was available (Warden et al., 2016a) and these data were transformed into TOC data (Dean, 1974).

3.3. Compound specific stable C isotope analysis

In order to constrain the source of brGDGTs in the sediments, we assessed their stable carbon isotope composition by analysis of their ether-bound alkyl moieties. To this end freeze-dried sediments from three different depth intervals from within the Ancylus Lake and Yoldia phases in sediment core 303600-N were pooled by equal amounts, homogenized in a mortar, and subsequently extracted by ASE and fractionated over Al_2O_3 as described above. The polar fractions were dissolved in hexane:isopropanol (99:1, v:v) and transferred to a column (4 cm) containing activated silica gel (3 h at 130 °C). The column was eluted with (1) hexane:isopropanol (96:4, v:v) and (2) hexane:isopropanol (90:10, v:v). The brGDGT-containing second fraction was dried and subjected to 57% HI in H_2O (Schouten et al., 1998) to cleave the ether bonds linking the alkyl chains with the glycerol backbone. The resulting alkyl iodides were reduced to hydrocarbons by H_2 in the presence of PtO_2 (Kaneko et al., 2011), and finally purified over activated Al_2O_3 by elution with hexane. The identity of the brGDGT-derived alkanes was confirmed by gas chromatography mass spectrometry (GC–MS) analysis and comparison of electron ionization (EI) mass spectra with previously published data (Sinninghe Damsté et al., 2000; Weijers et al., 2010; De Jonge et al., 2013; Weber et al., 2015). The ^{13}C content of the alkyl chains was determined by GC/combustion-isotope ratio mass spectrometry (GC/C-IRMS) using a Delta V™ Advantage IRMS (Thermo Scientific, USA). Samples were injected at 50 °C on a 50 m low-bleed Rxi®-5ms GC column (0.2 mm iD, 0.33 μm d_f, Restek, USA). After 2 min hold time, GC oven temperature was rapidly increased to 220 °C at 20 °C/min, held for 65 min to improve separation of alkanes and steranes, and finally increased at 4 °C/min to 320 °C (held for 35 min). The stable carbon isotopic composition of the analytes (reported in the δ-notation with respect to the V-PDB carbonate standard) were calibrated externally using an *n*-alkane mixture (C_{16}-C_{30}) with known isotopic compositions (mixture B3 provided by A. Schimmelmann, Indiana University, USA). GC/C-IRMS performance was monitored by regular analysis of this standard mixture. All samples were analyzed in triplicate.

3.4. Calculation of GDGT-based proxies

The Roman numerals refer to the GDGTs indicated in Fig. 1 and IV refers to crenarchaeol (Sinninghe Damsté et al., 2002). The 5-methyl brGDGTs and 6-methyl brGDGTs are distinguished by a prime on the latter and IV is crenarchaeol. The BIT Index was calculated including the 6-methyl brGDGTs as according to De Jonge et al. (2016):

$$\text{BIT index} = [(\text{Ia}) + (\text{IIa}) + (\text{IIIa}) + (\text{IIa}') + (\text{IIIa}')]/[(\text{Ia}) + (\text{IIa}) + (\text{IIIa}) + (\text{IIa}') + (\text{IIIa}') + (\text{IV})] \quad (1)$$

where (X) denotes the peak area of GDGT X (see Fig. 1) in the LC-MS analysis.

The isomer ratio (IR) signifies the quantity of the penta- and hexamethylated 6-methyl brGDGTs compared to the total brGDGTs (De Jonge et al., 2015a):

$$\text{IR} = ([\text{IIa}'] + [\text{IIb}'] + [\text{IIc}'] + [\text{IIIa}'] + [\text{IIIb}'] + [\text{IIIc}'])/([\text{IIa}] + [\text{IIb}] + [\text{IIc}] + [\text{IIa}'] + [\text{IIb}'] + [\text{IIc}'] + [\text{IIIa}] + [\text{IIIb}] + [\text{IIIc}] + [\text{IIIa}'] + [\text{IIIb}'] + [\text{IIIc}']) \quad (2)$$

where [X] denotes the fractional abundance of brGDGT X (see Fig. 1) based on the fractional abundances of all 15 brGDGTs that were quantified (i.e. excluding IIIa″).

The MBT'_{5me} was calculated according to De Jonge et al. (2014a):

$$\text{MBT}'_{5\text{me}} = ([\text{Ia}] + [\text{Ib}] + [\text{Ic}])/([\text{Ia}] + [\text{Ib}] + [\text{Ic}] + [\text{IIa}] + [\text{IIb}] + [\text{IIc}] + [\text{IIIa}]) \quad (3)$$

The weighted-average of cyclopentane moieties was calculated for the tetra- and pentamethylated brGDGTs according to Sinninghe Damsté (2016):

$$\#\text{rings}_{\text{tetra}} = ([\text{Ib}] + 2 * [\text{Ic}])/([\text{Ia}] + [\text{Ib}] + [\text{Ic}]) \quad (4)$$

$$\#\text{rings}_{\text{penta5me}} = ([\text{IIb}] + 2 * [\text{IIc}])/([\text{IIa}] + [\text{IIb}] + [\text{IIc}]) \quad (5)$$

$$\#\text{rings}_{\text{penta6me}} = ([\text{IIb}'] + 2 * [\text{IIc}'])/([\text{IIa}'] + [\text{IIb}'] + [\text{IIc}']) \quad (6)$$

The average number of rings of the tetra- and pentamethylated brGDGTs was calculated as follows:

$$\#\text{rings} = \left([\text{Ib}] + [\text{IIb}] + [\text{IIb}'] + 2 * ([\text{Ic}] + [\text{IIc}] + [\text{IIc}'])\right) / \left([\text{Ia}] + [\text{Ib}] + [\text{Ic}] + [\text{IIa}] + [\text{IIb}] + [\text{IIc}] + [\text{IIa}'] + [\text{IIb}'] + [\text{IIc}']\right) \quad (7)$$

The soil-based CBT′ and MBT'_{5Me} calibrations were used for the calculation of pH and MAT (De Jonge et al., 2014a):

$$CBT' = {}^{10}\log\left[(Ic + IIa' + IIb' + IIc' + IIIa' + IIIb' + IIIc')/(Ia + IIa + IIIa)\right] \quad (8)$$

$$pH = 7.15 + 1.59 * CBT' \quad (9)$$

$$MAT = -8.57 + 31.45 * MBT'_{5Me} \quad (10)$$

The marine bottom water temperature (BWT) calibration designed for coastal marine sediments was calculated according to Dearing Crampton Flood et al. (2018):

$$BWT = 59.5 * MBT'_{5me} - 23.7 \quad (11)$$

Mean annual air temperature (MAT) was calculated using a novel calibration created using sediments from East African lakes (Russell et al., 2018):

$$MAAT = -1.2141 + 32.4223 * MBT'_{5Me} \quad (12)$$

3.5. Statistical analysis

Principal component analysis (PCA) was executed using Sigmaplot© version 13. The statistical analysis was performed using the fractional abundances of all 15 of the 5- and 6-methyl brGDGTs for the entire set of sediments (n = 237).

4. Results

The two sediment cores from the central Gotland Basin together comprise a record composed of the last part of the Yoldia Sea phase, the Ancylus Lake and the brackish phases (see Sollai et al., 2017 for details). Their TOC content varied from ca. 3 to as high as 16% in the recent brackish phase (from 7.2 cal kyr BP to the present; see Warden et al., 2017), while it was substantially lower (i.e. <2%) in the Ancylus Lake and Yoldia Lake phases (Fig. 3a; Sollai et al., 2017). The two Arkona Basin cores provided a record starting in the Baltic Ice Lake period up to the recent brackish period (see Warden et al., 2016a). The sedimentary loss on ignition (LOI) content varied from ca. 11% to as high as 17.7% in the recent brackish phase, while it was substantially lower (i.e. 5.5% on average) in the Ancylus Lake phase (Fig. 4a). For the sediments deposited during the start of the Ancylus Lake phase, the Yoldia Sea phase, and the Baltic Ice Lake period no LOI data are available.

4.1. Concentration and distribution of GDGTs

The summed brGDGT concentrations (normalized to the TOC content) in both the Gotland and Arkona Basin sedimentary records during the brackish phase were substantially lower than during the Ancylus Lake and preceding phases (Figs. 3b and 4b). The crenarchaeol concentration was highly variable but the average amounts were similar in the Ancylus Lake and the brackish phases of both basins (Figs. 3 and 4). The same holds true for the concentration of GDGT-0, which was also highly variable and the amounts were similar in both the Ancylus Lake and brackish phases in both the Gotland and Arkona basins. In the brackish phase of the Gotland Basin record, lower concentrations of both crenarchaeol and summed brGDGTs occured in low TOC sediments (Fig. 3), i.e. at times when bottom water were oxic. This may be related to decreased preservation under oxic conditions.

The relative abundances of the three major classes of GDGTs, i.e. summed brGDGTs, crenarchaeol, and GDGT-0 (cf. Blaga et al., 2009), showed substantial variation (Fig. 5). Included in this plot are data from BS surface sediments and those of the nearby Skagerrak (for which no absolute concentration data are available). All but one had relatively low brGDGT abundances and fall in the same area as those of the brackish phase sediments of the Gotland and, to a lesser extent, Arkona Basin. Such GDGT distributions are typical for marine sediments (Schouten et al., 2013). The sediments of the Ancylus Lake, the Yoldia Sea, and Baltic Ice Lake phases from both basins contained substantially higher relative amounts of brGDGTs (i.e. >20%; Fig. 5) with one exception (in the Ancylus Lake phase of the Gotland Basin).

These changes translated into distinct differences in the BIT index. The BIT index was low for both the Skagerrak (0.08 ± 0.02) and BS surface sediments (0.06 ± 0.09). However, a Bothnian Sea surface sediment (377850; Fig. 2) stood out with a substantially higher value, i.e. 0.31. For the Gotland Basin record, the BIT index decreased from the Ancylus Lake (0.44 ± 0.16) to the brackish phase (0.06 ± 0.02) (Fig. 3d). The brackish phase values are close to those of most BS surface sediments. For the Arkona Basin record, the BIT index was high in the Baltic Ice Lake (0.79 ± 0.03), Yoldia Sea (0.77 ± 0.05) and Ancylus Lake (0.74 ± 0.08) phases and declined again in the brackish phase (0.17 ± 0.02) (Fig. 4d) but not as pronounced as for the Gotland Basin.

4.2. brGDGT distributions

All 15 brGDGTs (see Fig. 1 for structures) identified previously in soils and marine sediments with the UHPLC-MS method (e.g. De Jonge et al., 2013; Warden et al., 2016b; Sinninghe Damsté, 2016) were detected. Similar brGDGT distributions were observed in the BS and Skagerrak surface sediments (Fig. 6c and f) and the brackish phase sediments from both basins (Fig. 6a and b). The brGDGT distributions during the Ancylus Lake and Yoldia Sea phases of the Gotland and, to a lesser extent, Arkona basins were characterized by a much higher fractional abundance of brGDGTs IIIa and IIIa′ than in the brackish phase (Fig. 6). The Ancylus Lake phase of the Gotland Basin had the highest average fractional abundance of brGDGT IIIa′ (0.31 ± 0.08) of all sediments (Fig. 6e). The Ancylus Lake phase of the Gotland Basin and the Baltic Ice Lake phase of the Arkona Basin had the highest average fractional abundance of brGDGT IIIa (~0.34) (Fig. 6e and h). All of the lower salinity phase sediments from both basins (Ancylus Lake, Yoldia Sea, and Baltic Ice Lake phases) were dominated by non-cyclic brGDGTs (Fig. 6e–h) in contrast to those of higher salinity phases such as the BS and Skagerrak surface sediments, and those of the Arkona Basin brackish phase (Fig. 6a–d).

To determine the factors controlling the brGDGT distribution in all sediments (n = 237), PCA was performed on the fractional abundances of the 15 brGDGTs. PC1 explained 46% of the total variance and appeared to be predominantly related to the degree of methylation of brGDGTs, as the most abundant hexamethylated brGDGTs (IIIa, IIIa′, IIIb, IIIc) plotted negatively on PC1 and most of their less methylated counterparts (Ia, Ib, Ic, IIa, IIa′, IIb, IIb′, IIc, IIc′) plotted positively (Fig. 7a). For the overall sample set, the sample score on PC1 was highly positively correlated ($R^2 = 0.91$) with the MBT'_{5Me} (see Eq. (3)), a measure of the degree of methylation of the 5-methyl brGDGTs (De Jonge et al., 2014a). PC2 explained 20% of the variance and was related to the fractional abundance of the 5- versus 6-methyl brGDGTs. All 6-methyl brGDGTs scored positively on PC2, whereas the most abundant 5-methyl brGDGTs (i.e. Ia, IIa, and IIIa) scored negatively on PC2 (Fig. 7a). Indeed, the sample score on PC2 correlated negatively with the IR (see

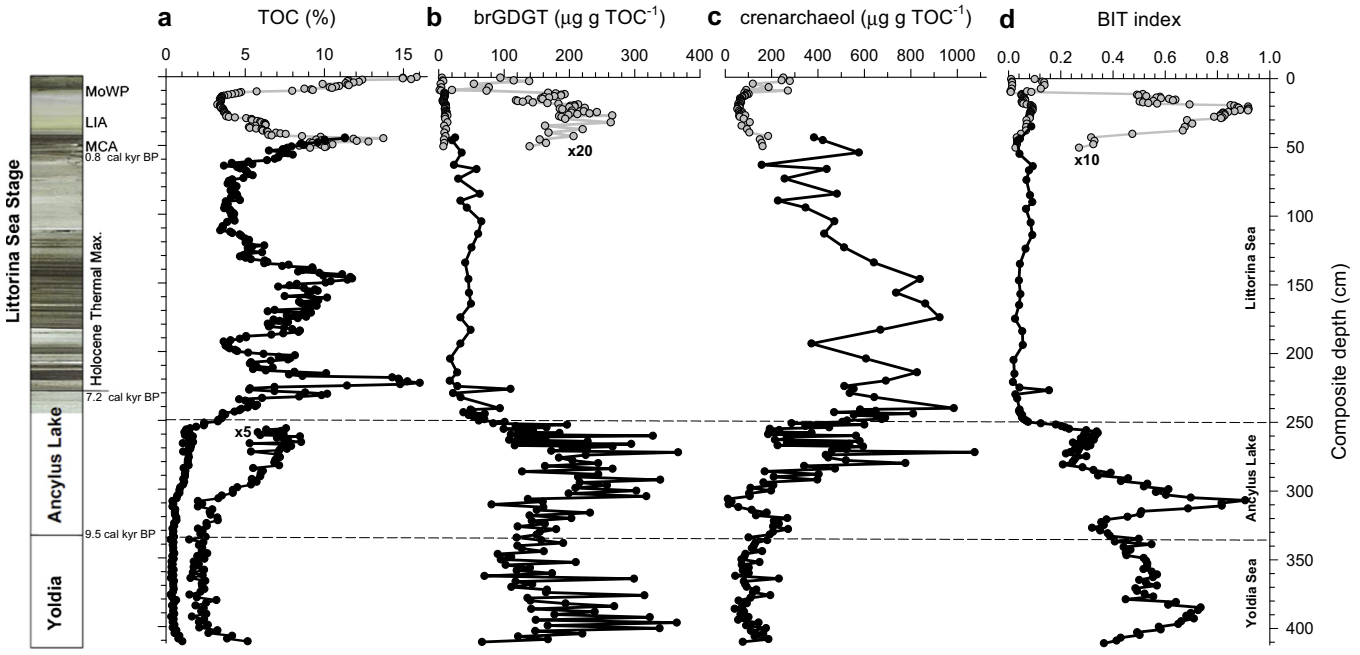

Fig. 3. The Gotland Basin sedimentary record showing variations with depth for (a) TOC content (data from Sollai et al. (2017) and Warden et al. (2017)), (b and c) concentrations of summed brGDGTs and crenarchaeol (in µg g^{-1} TOC), and (d) the BIT index. The stratigraphy of the sections following Sollai et al. (2017) is given. Multicore P435-1-4 and core 303600-N sediments are plotted in grey and black circles, respectively.

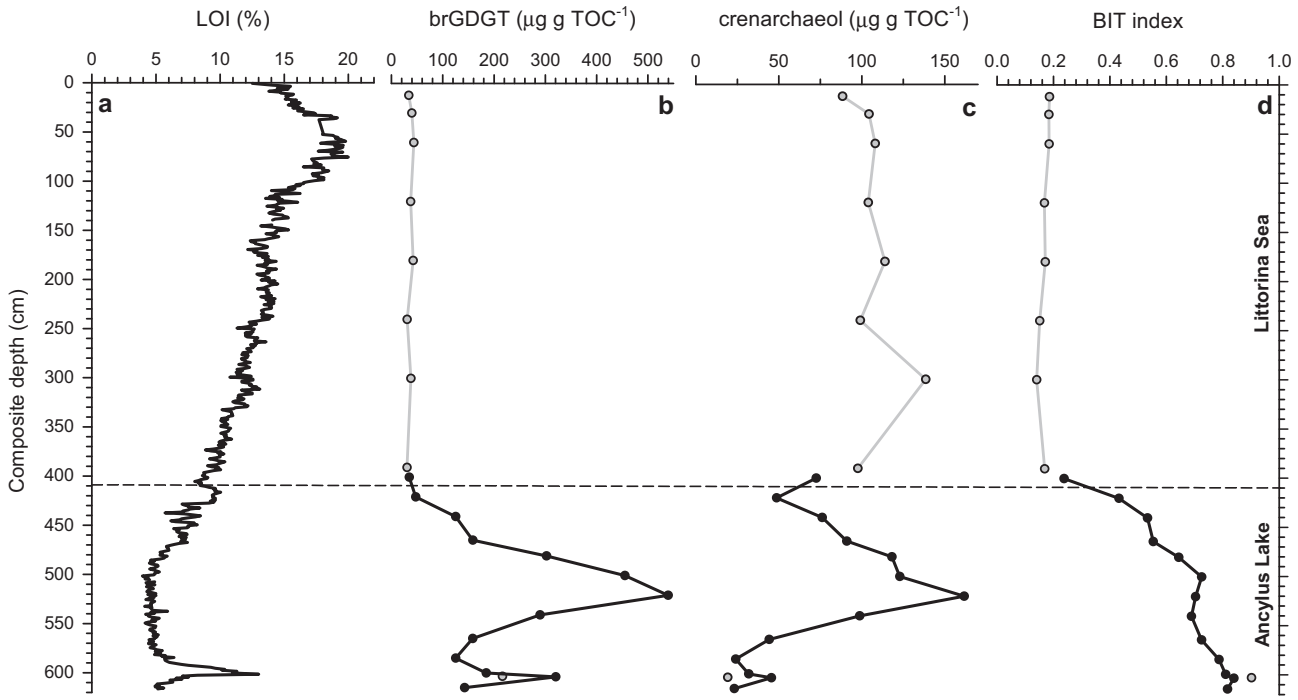

Fig. 4. The Arkona Basin sedimentary record showing variations with depth for (a) LOI content (data from Warden et al., 2016a), (b and c) concentrations of summed brGDGTs and crenarchaeol (in µg g^{-1} TOC), and (d) the BIT index. The stratigraphy of the sections following Warden et al. (2016a) is given. There is no available LOI data to normalize the concentrations of the GDGTs for the Baltic Ice Lake and Yoldia See phases so only data for the upper part of the section is shown. Data for the BIT index for the deeper section is provided in Fig. 9. Core 31810 and 318340 sediments are plotted in grey and black circles, respectively.

Eq. (2)) (R^2 = 0.61), which is a reflection of the relative abundance of the 6-methyl brGDGTs (De Jonge et al., 2014b). PC3 explained 9% of the variance. Ia, IIa, and IIa′ scored negatively on this PC, whilst almost all cyclic tetra- and pentamethylated brGDGTs (i.e. Ib, Ic, IIb, IIc, and IIc′) scored positively (Fig. 7c). The sample score on PC3 is negatively correlated (R^2 = 0.45) with the average number of rings of the tetra- and pentamethylated brGDGTs (#rings, see Eq. (7)). The correlation coefficient increased to 0.78 when only the surface sediments and sediments of the brackish phase are considered. The significant correlations of the three PCs with the molecular ratios of brGDGTs for the degree of methylation and cyclisation and the relative abundance of 6-methyl brGDGTs indicate that they provide a good description of the variance in the dataset.

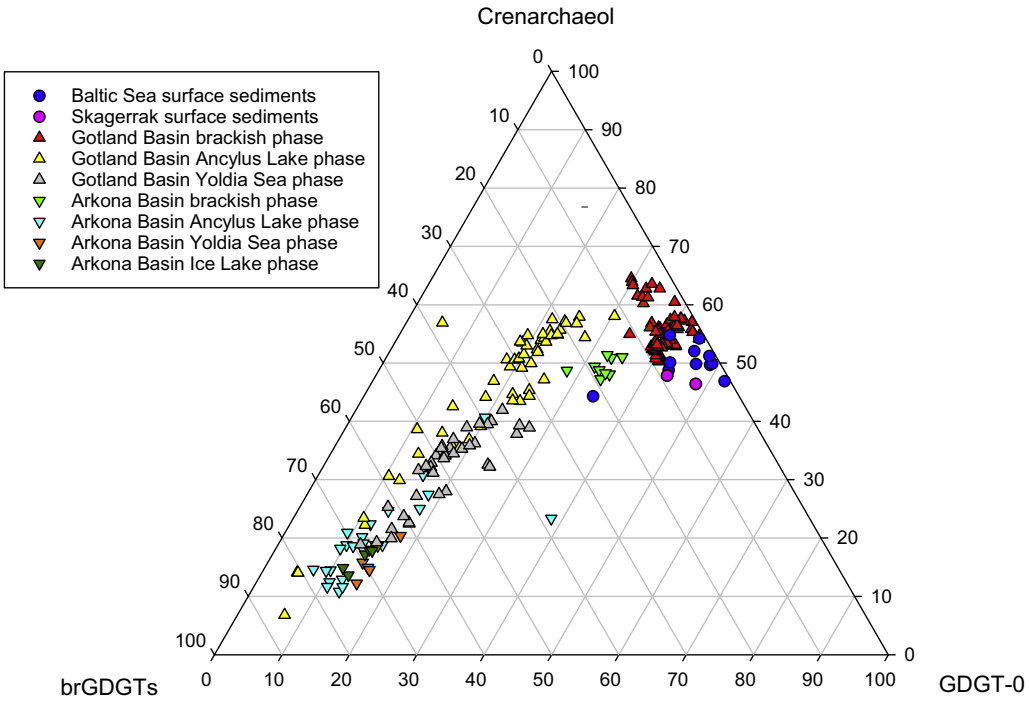

Fig. 5. Ternary diagram (after Blaga et al., 2009) illustrating the composition of the major isoprenoid (GDGT-0 and crenarchaeol) and the summed brGDGTs in the BS sediments used in this study. The sediments from different locations and phases are represented by symbols with different colors and shapes as indicated. (For interpretation of the references to colour in this figure legend, the reader is referred to the web version of this article.)

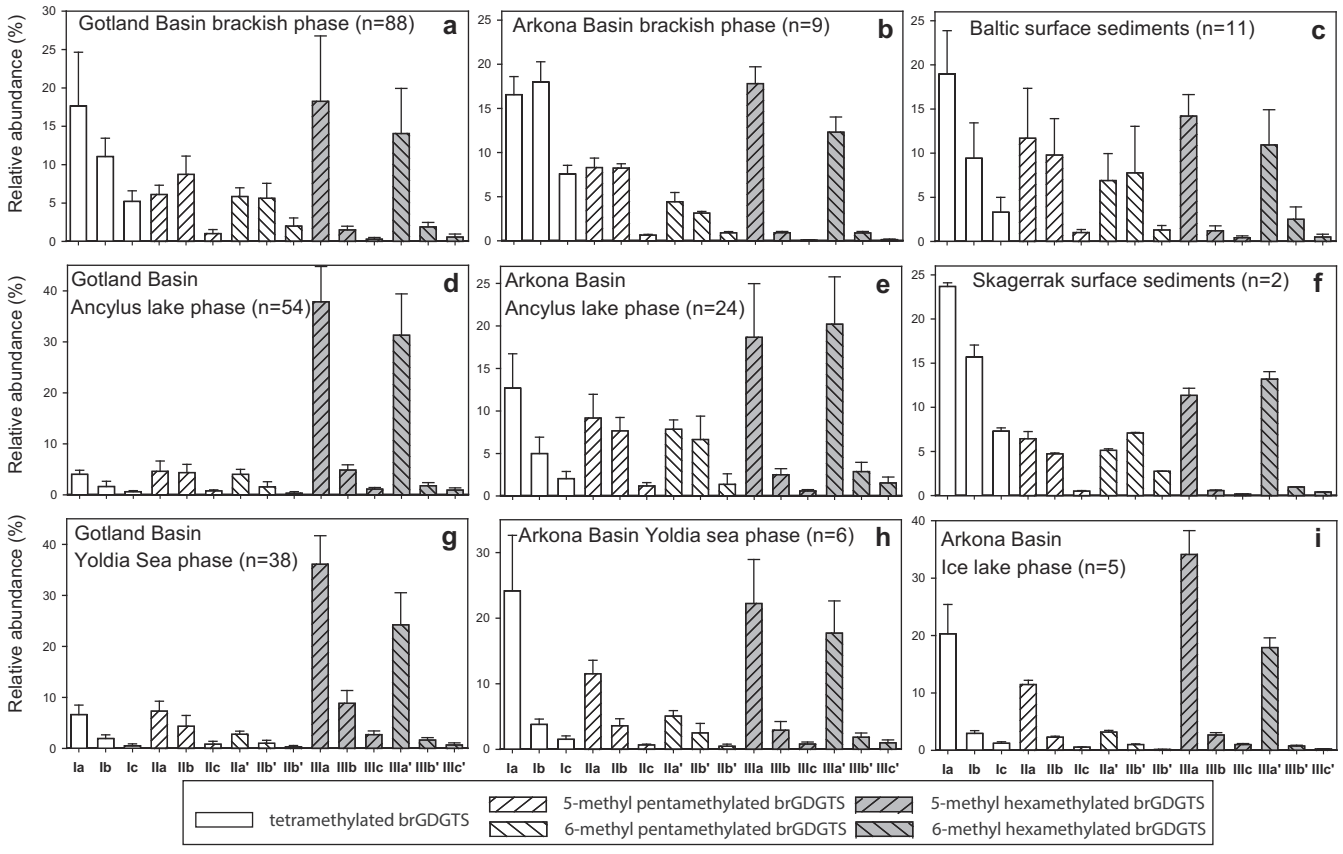

Fig. 6. The average brGDGT distribution for the (a) brackish, (d) Ancylus Lake, (g) and Yoldia Sea phases of the Gotland Basin, the (b) brackish, (e) Ancylus Lake, (h) Yoldia Sea, and (i) Ice Lake phases of the Arkona Basin, and the surface sediments of the (c) BS and (f) Skagerrak. The error bars indicate the standard deviation in the individual fractional abundances. The various groups of brGDGTs are discerned by different fillings of the bars. Note that the scale for the fractional abundance of the various plots varies.

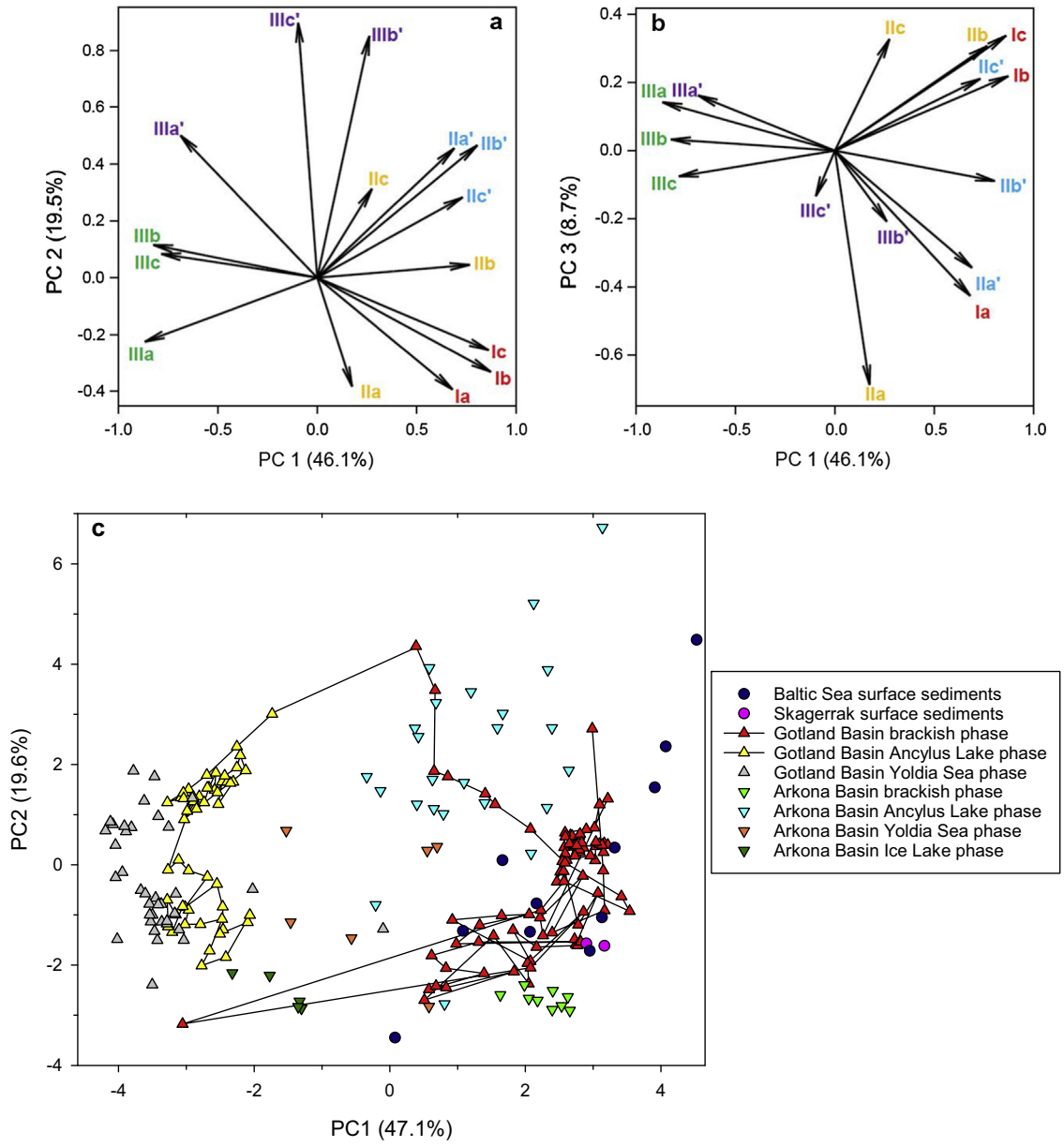

Fig. 7. Results of principal component analysis (PCA) based on the fractional abundances of the 15 brGDGTs in 237 sediments from the BS, showing (a-b) variable loadings and (c) sample score on PC1 and PC2. The Roman numerals refer to brGDGT structures (Fig. 1) and are color coded for groups of structurally related brGDGTs. The different sample sets in (c) are designated by symbols with different color and shape as indicated. The depth trend in the Gotland Basin core of the brackish and Ancylus Lake phases is visualized by connecting adjacent sediment layers. (For interpretation of the references to color in this figure legend, the reader is referred to the web version of this article.)

The surface and brackish phase sediments scored positively on PC1 but show substantial variation on PC2 (Fig. 7c). The BS surface sediments that scored negatively on PC2 were mostly those from the northern part of the basin (i.e. 372820, 377850, 377830, 349200 and 349190) and those in the south that were close to the connection with the North Sea (372720 and 303600) as well as the Skagerrak surface sediments. All Ancylus Lake and Yoldia Lake phase sediments from the Gotland Basin scored negatively on PC1 as did all of the sediments of the Baltic Ice Lake phase from the Arkona Basin, albeit to a lesser extent (Fig. 7c). Again there is quite some variation in the score on PC2. The Yoldia Sea phase sediments from the Arkona Basin plot in between these groups, whilst sediments from the Arkona Basin Ancylus Lake phase plot predominantly in the upper quadrant of the score plot (Fig. 7c). The Gotland Basin high-resolution record clearly reveals a gradual change in the brGDGT distribution as indicated by the line connecting adjacent sediment layers (Fig. 7c); at the boundary between the brackish and Ancylus Lake phases the score on PC2 is the highest of the entire dataset.

The novel brGDGT IIIa″ (Fig. 1), which has been linked to lacustrine in situ brGDGT production (Weber et al., 2015), was almost constantly present during the Ancylus Lake and Yoldia Sea phases of both the Gotland (Fig. 8d) and Arkona Basin (Fig. 9d) sedimentary records but absent in the brackish period. The upper part of the Gotland Basin Ancylus Lake phase lacked IIIa″. It was also not detected in the Baltic Ice Lake phase of the Arkona Basin (Fig. 9d).

4.3. Stable carbon isotopic composition of brGDGTs

To shed light on potential brGDGT sources, we examined their ^{13}C content in core sections with a high fractional abundance of brGDGT IIIa″ by ether cleavage and GC-IRMS analysis of their alkyl chains (see experimental). It was not possible to obtain individual $\delta^{13}C$ data for the 5,13,16- and 6,13,16-trimethyloctacosanes

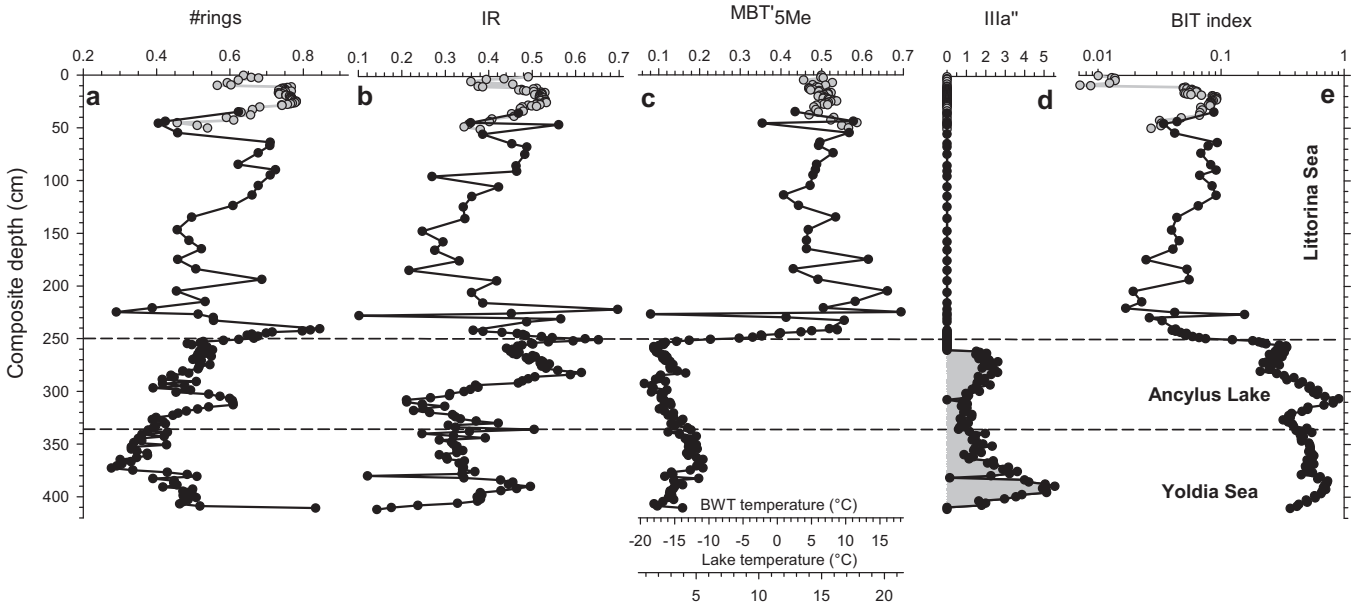

Fig. 8. Variations in brGDGT molecular ratios for the Gotland Basin plotted on a composite depth scale: (a) #rings, (b) IR, (c) MBT'_{5Me}, (d) the relative abundance of IIIa″, and (e) the BIT index. The relative abundance of IIIa″ is expressed as the % contribution of IIIa″ to the sum of the non-cyclic hexamethyl brGDGTs IIIa, IIIa′, and IIIa″. The stratigraphy of the sections following Sollai et al. (2017) is given. The samples of multicore P435-1-4 and gravity core 303600-N are plotted in grey and black circles, respectively. The BIT index is plotted on a log scale.

(which were only partly separated by GC); when integrated together resulting $\delta^{13}C$ values were identical to that of 13,16-dimethyloctacosane (Table 2).

5. Discussion

5.1. Provenance of brGDGTs

The application of brGDGTs on marine and lake sediments for paleoclimate studies can be complicated when diverse sources of brGDGTs exist. These sources include soils (Weijers et al., 2007a; Bendle et al., 2010), peats (Weijers et al., 2006a), and lacustrine (Buckles et al., 2014), riverine (Yang et al., 2013; Zell et al., 2013; De Jonge et al., 2014b; Warden et al., 2016b), and marine (Peterse et al., 2009; Weijers et al., 2014; Sinninghe Damsté, 2016) in situ production. Therefore, the major sources should be assessed before using brGDGTs for paleoenvironmental purposes (e.g. Yang et al., 2013; Zell et al., 2013; De Jonge et al., 2015b; Warden et al., 2016b).

The ternary plot of the major GDGTs (Fig. 5), along with the BIT index, the summed brGDGTs and crenarchaeol concentrations (Figs. 3 and 4), and brGDGT distribution (Figs. 8 and 9) all demonstrated that the sedimentary GDGT composition was highly dependent on the varying environmental conditions in the BS over the Holocene. The Baltic Ice Lake, Yoldia Sea and Ancylus Lake phases show higher values for the BIT index, whereas it is substantially lower during the brackish phase (Figs. 3d and 4d). The records of crenarchaeol and summed brGDGTs concentration indicate that for both basins the decline of BIT index values is predominantly caused by the much reduced brGDGT concentration in the brackish phase (Figs. 3d and 4d). This decrease goes together with a substantial change in the brGDGT composition as is evident from the PCA analysis (Fig. 7). This change in brGDGT provenance is the most remarkable and consistent event in both the Gotland and Arkona Basin GDGT records and roughly co-occurs with the increased marine influence corresponding with the opening of the Danish Straits, which allowed inflow of marine water into the BS (Winterhalter, 1992; Andrén et al., 2000a, 2000b). Indeed, these co-occurring changes start at the end of the Ancylus Lake phase, which is characterized by a consistent decreasing trend in the BIT index and rapid changes in the brGDGT molecular ratios (Figs. 8 and 9). When the BIT index was introduced more than a decade ago, it was interpreted to reflect soil organic matter input (of which a value close to 1 indicates a predominant soil origin and a value close to zero indicates a marine origin; Hopmans et al., 2004). However, in situ brGDGT production in rivers (Yang et al., 2013; Zell et al., 2013; 2014; De Jonge et al., 2014b) and lakes (Tierney and Russell, 2009; Sinninghe Damsté et al., 2009; Loomis et al., 2011; Buckles et al., 2014) can also result in a high BIT index. Therefore, the high BIT index values in the pre-brackish phases do not necessarily indicate a substantially enhanced input of soil organic matter. To examine the potential brGDGT sources, we will discuss their provenance in detail. Various lines of evidence suggest that autochthonous brGDGT production played an important role in the BS during the Holocene and shall be discussed below.

5.1.1. The brackish phase

In the Gotland Basin the brGDGT concentration is low compared to the aquatic crenarchaeol production by Thaumarchaeota resulting in a generally low BIT index (<0.10; Fig. 3d). These minor brGDGTs could derive from either soil erosion or in situ production. Sinninghe Damsté (2016) discussed how these dual sources of brGDGTs complicated their paleoclimatic application in coastal marine sediments and showed that in situ brGDGT production is widespread at water depths of 50–300 m, likely due to the higher delivery of organic matter. Sinninghe Damsté (2016) explored several methods for determining the brGDGT provenance in such settings. Since the average depth of the BS is 54 m and the water depth of the core locations are 175 (Gotland Basin) and 46 m (Arkona basin), sedimentary in situ brGDGT production must be assessed.

Sinninghe Damsté (2016) demonstrated that when the fractional abundances of the tetra-, penta- and hexamethylated brGDGTs from soils were plotted in a ternary diagram, the data points lie within a distinct area. By comparing brGDGTs in coastal sediments with soils, it can be assessed whether the brGDGTs are

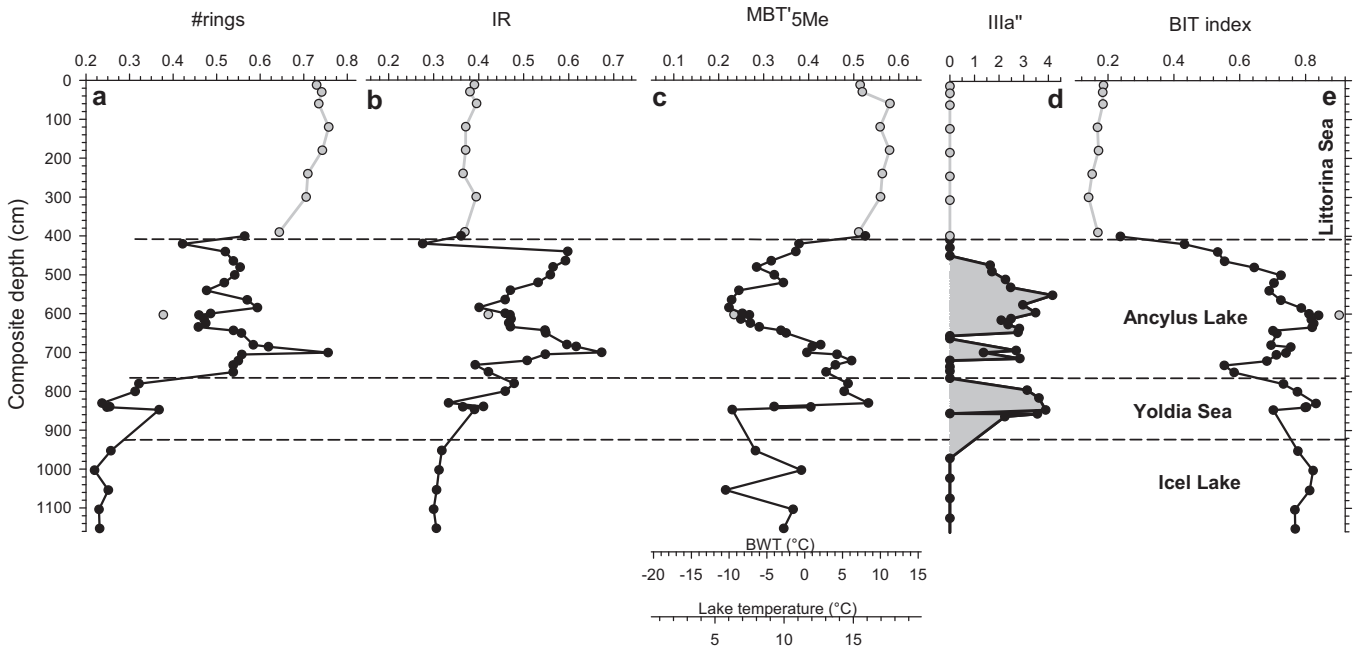

Fig. 9. Variations in brGDGT molecular ratios for the Arkona Basin plotted on a composite depth scale: (a) #rings, (b) IR, (c) MBT′$_{5Me}$, (d) the relative abundance of IIIa″, and (e) the BIT index. The relative abundance of IIIa″ is expressed as the % contribution of IIIa″ to the sum of the non-cyclic hexamethyl brGDGTs IIIa, IIIa′, and IIIa″. The stratigraphy of the sections following Warden et al. (2016a) is given. The samples of multicores 318310 and 318340 are plotted in grey and black circles, respectively.

Table 2
The $\delta^{13}C$ values of brGDGTs and TOC from selected sediment depths from core 303600-N from the Gotland Basin.

Sediment depth (cm)	brGDGT-derived alkane(s)	$\delta^{13}C$[a] (‰)	$\delta^{13}C_{TOC}$ (‰)
234–243	13,16 dimethyloctacosane (a)	−28.4 ± 0.3	−28.1 ± 0.1
	5,13,16- and 6,13,16 trimethyloctacosane (b + c)	−29.0 ± 0.0	
309–323	13,16 dimethyloctacosane (a)	−28.8 ± 0.3	−27.7 ± 0.4
	5,13,16 and 6,13,16 trimethyloctacosane (b + c)	−28.7 ± 0.1	
351–363	13,16 dimethyloctacosane (a)	−27.4 ± 0.1	−26.3 ± 0.2
	5,13,16 and 6,13,16 trimethyloctacosane (b + c)	−28.4 ± 0.1	

[a] Average and standard deviation based on analysis in triplicate.

predominantly derived from soils through input from land (e.g. by riverine transport) or from aquatic (in situ) production. Few brackish phase BS sediments plot on top of the global soil data set (Fig. 10), suggesting that the brGDGTs are not predominantly derived from soil.

The number of rings of the tetramethylated and the 5- and 6-methyl pentamethylated brGDGTs (#rings$_{tetra}$, #rings$_{penta\ 5Me}$, and #rings$_{penta\ 6Me}$; see Eqs. (4)–(6)) is another way of detecting in situ production in marine sediments (Sinninghe Damsté, 2016). Most of the surface and brackish phase sediments have the highest values for #rings$_{tetra}$, #rings$_{penta\ 5Me}$, and #rings$_{penta\ 6Me}$ (Fig. 10). To simplify the discussion we will focus on the average number of rings of the tetra- and pentamethylated brGDGTs (#rings, see Eq. (7)). The degree of cyclization of brGDGTs is predominantly controlled by pH (Weijers et al., 2007a; Peterse et al., 2010). The high #rings in Svalbard fjord (i.e. 0.8–1.0) and other coastal marine sediments have consequently been interpreted to be predominantly the consequence of in situ production in alkaline sedimentary pore waters (Peterse et al., 2009; Sinninghe Damsté, 2016). For BS and Skagerrak surface sediments #rings ranges between 0.44 and 0.72 (average 0.60 ± 0.09), excluding sample 377850 located in the lower Bothnian Sea as the outlier (0.11). This suggests that most surface sediments in situ production was important and the contribution of soil-derived brGDGTs has been low. High #rings values (i.e. 0.6–0.7) have also been observed in alkaline soils (Sinninghe Damsté, 2016) and thus erosion could also be the cause. However, the often peat covered soils of the continent surrounding the BS basin are slightly acidic. The average pH is 6.1 for soils (0–25 cm depth) collected from 10 countries surrounding the BS basin (Reimann et al., 2000). Additionally, high pH soils tend to have high amounts of 6-methyl brGDGTs (IR > 0.7; De Jonge et al., 2014b) and the BS surface sediments have a much lower average IR (0.47 ± 0.10; Figs. 8 and 9), also pointing towards insignificant input of alkaline soils. Hence, the #rings can be used as an indicator for in situ production and where values exceed 0.7 (value indicated by the gray dotted lines in Fig. 11) a predominant origin from in situ production can be assumed.

The exceptional Bothnian Sea surface sediment 377850 with the low #rings (0.11) also had a much higher BIT index (0.31) compared to all other surface sediments. Kaiser and Arz (2016) compared brGDGT and leaf-wax *n*-alkane concentrations in BS surface sediments and concluded that the BIT index does reflect the relative contribution of soil organic matter. They also reported a high soil organic matter input into the Bothnian Sea (average 29%), in agreement with lignin phenol data indicating a 30% terrestrial organic matter contribution in the northern BS (Bianchi et al., 1997). The low #rings (0.11) and low IR (0.34) values of the brGDGTs in surface sediment 377850 are in agreement with the low pH of soils surrounding the BS. Using this sediment as an end-member of soil derived brGDGTs in the BS region and a #rings

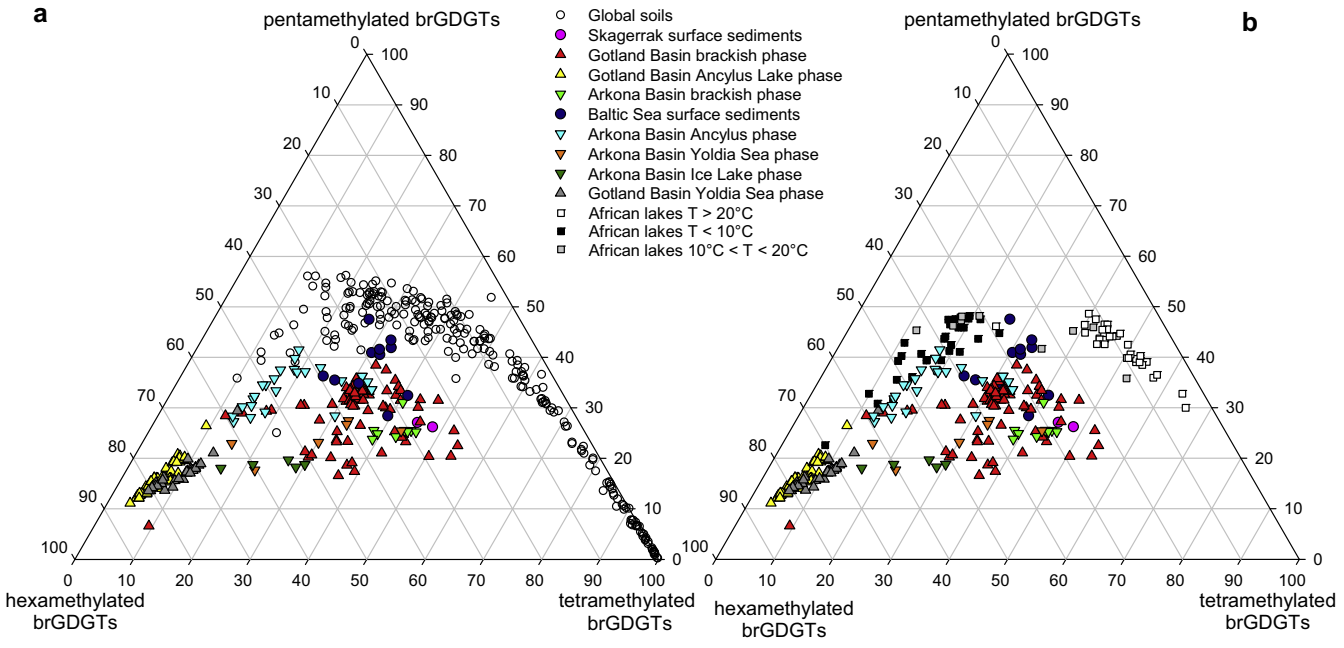

Fig. 10. (a) Ternary diagram illustrating the fractional abundances of the tetra- (Ia-c), penta (IIa-c and II′a-c), and hexamethylated (IIIa-c and III′a-c) brGDGTs. The global soil dataset (open circles; De Jonge et al., 2014a) is included for reference. The different basins and different phases of sedimentation are shown by symbol and color as indicated. Only one of the BS sediments (i.e. 377850, which also has the highest BIT index, see text) plots clearly on top on the global soil data, demonstrating that for almost all sediments the brGDGTs were not 100% soil-derived (cf. Sinninghe Damsté, 2016). Only a few BS surface sediments and some sediments from the Ancylus Lake phase of both basins plot relatively close to the global soil dataset, indicating these sediments may have received a contribution from terrestrially derived brGDGTs. (b) Same but now the African Lake data set (squares; data from Russell et al., 2018) subdived on the basis of lake temperature ranges is plotted for reference. Various datasets plot (i.e. Ancylus Lake phase for Arkona and Gotland Basins, Yoldia Sea phase Gotland Basin) close to the data points for lakes with a temperature <10 °C, indicating that these brGDGT distributions are consistent with a "cold lake distribution". (For interpretation of the references to colour in this figure legend, the reader is referred to the web version of this article.)

value of 0.8 for in situ produced brGDGTs (Sinninghe Damsté, 2016) suggests that 70 ± 13% of the brGDGTs in the other surface sediments is in situ produced.

The Gotland Basin brGDGT distribution in the brackish phase sediments reveals that they also must be primarily derived from in situ production. The brGDGT abundance relative to crenarchaeol is always low (BIT index <0.10; Fig. 3d), caused by low absolute brGDGT concentrations (Fig. 3b). At the same time, #rings values are variable but generally high (0.4–0.75) and in certain intervals even approach or exceed the value of 0.8 that indicates an exclusive origin from in situ production. The brGDGT distribution during this phase remains relatively constant as revealed by the PCA score plot (Fig. 7c) and the relatively constant values for MBT'_{5Me} of around 0.5 (Fig. 8c). Higher values for MBT'_{5Me} and lower values for #rings are seen in higher TOC sediments (i.e. Medieval Climate Anomaly (MCA) and Holocene thermal maximum; Fig. 8a). Similar observations are made for the Arkona Basin brackish phase record (Figs. 4 and 9), where #rings is 0.70 ± 0.06 and MBT'_{5Me} is 0.55 ± 0.03. The values for the BIT index are slightly higher (0.18 ± 0.03) than in the Gotland Basin (Fig. 3), but this is probably due to the lower crenarchaeol concentration rather than due to increased brGDGT concentrations (Fig. 4). The increased crenarchaeol concentration in the Gotland Basin brackish phase sediments may be related to the strong stratification of its water column. A study of the Black Sea, a large, stratified body of water with anoxic bottom waters and abundant sulfide below 100 m, demonstrated that crenarchaeol-producing Thaumarchaeota are abundant in the suboxic zone (Coolen et al., 2007). Similarly, the Gotland Basin has also been persistently stratified with an oxic upper layer and anoxic bottom waters (e.g. Suess, 1979; Sternbeck and Sohlenius, 1997), sustaining a chemocline and supporting a population of Thaumarchaeota (Berg et al., 2015) conducive to higher crenarchaeol production.

The high resolution Gotland Basin MUC record shows the influence of bottom water oxygen concentration on the GDGT distribution. This core covers the MCA and Modern Warm Period (MWP), both characterized by relatively high TOC contents and laminated sediments (Fig. 3). The Little Ice Age (LIA), which occurs between these two periods, is characterized by homogenous sediments and a substantially lower TOC content (Kabel et al., 2012). The highest BIT index values, although still low (<0.1; see inset in Fig. 3b), coincides with the interval with the lowest TOC values, likely indicating this period had the highest oxygen bottom water concentrations. The brGDGT and crenarcheaol concentration profiles (Fig. 3b and c) show that the increase in the BIT index is mostly due to the decrease in crenarchaeol concentration. This could be explained by a reduced preservation of crenarchaeol produced in the water column. The #rings is also highest in the interval with the highest BIT index values (Fig. 8). This would be consistent with the idea that these brGDGT are predominantly produced in the surface sediments, which would promote their preservation. This has no major impact on the degree of methylation since MBT'_{5Me} remains fairly constant (Fig. 8).

Down core in the Gotland Basin record, larger changes in the MBT'_{5Me} profile are observed (Fig. 8c). The increases in MBT'_{5Me} occur in sediments with a high TOC content and are caused by a large increase in the fractional abundance of brGDGT Ia and co-occur with a substantial drop in #rings (Fig. 8a). In fact, a significant linear correlation ($R^2 = 0.88$) exists between [Ia] and #rings for the entire brackish interval. The endmember in this respect is the sediment at 225 cm, which has values for MBT'_{5Me}, [Ia] and #rings of 0.69, 0.44, and 0.29, respectively. This strongly suggests that under anoxic bottom water conditions in situ production in the sediments is suppressed, and brGDGTs from another source become relatively important. Soil-derived brGDGTs would be a possibility, but the overall brGDGT composition of these sediments

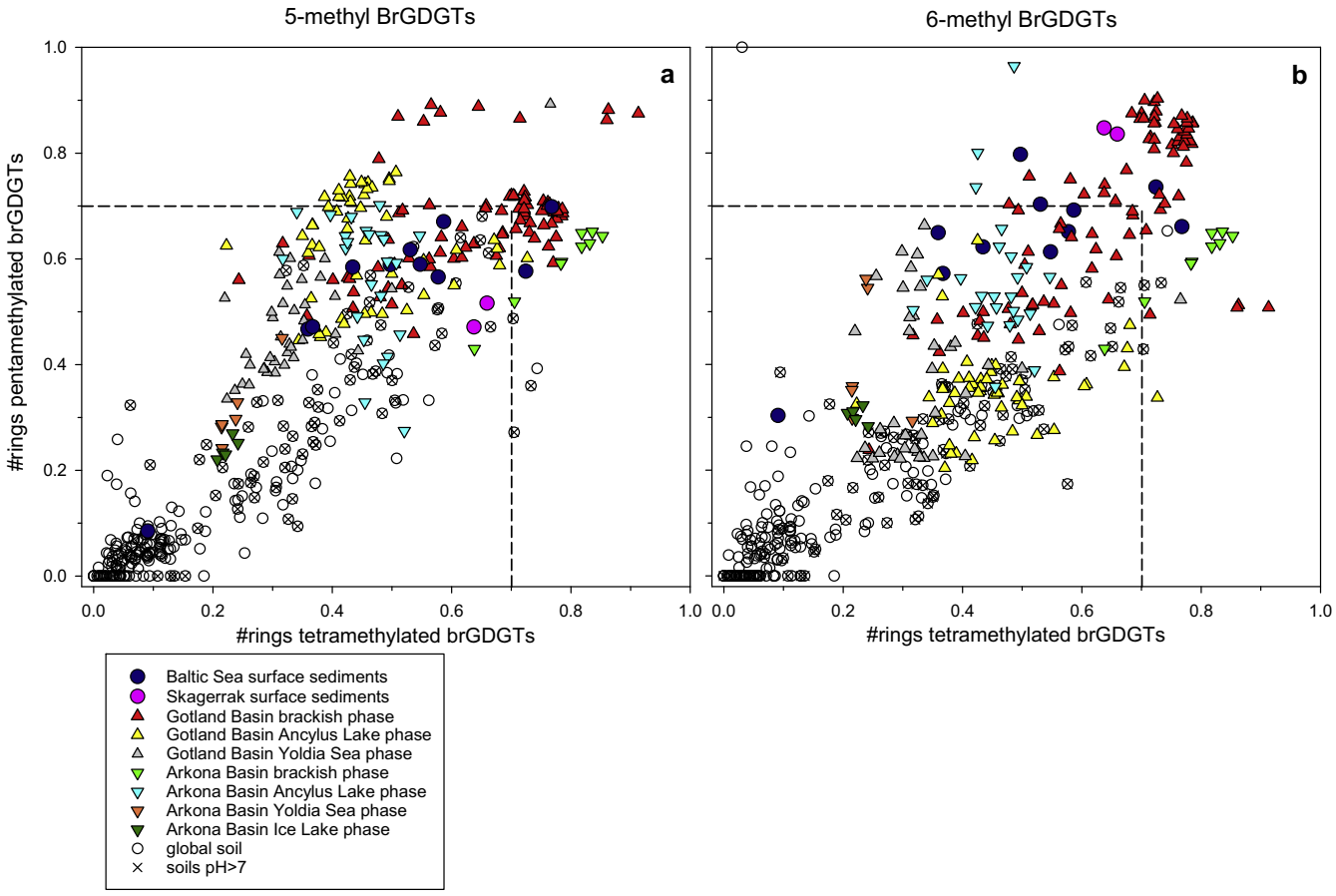

Fig. 11. Scatter plots of the number of cyclopentyl rings (#rings) in the tetramethylated brGDGTs (calculated using Eq. (4)) vs. (a) 5-methyl pentamethylated brGDGTs (calculated using Eq. (5)), and (b) 6-methyl pentamethylated brGDGTs (calculated using Eq. (6)). The different basins and different phases of sedimentation are shown by symbol and color as indicated. Soils from the global data set are plotted for reference; those with a pH > 7 are indicated with an 'x' (data from De Jonge et al., 2014a). The data reveal that sediments deposited during the brackish phase in both the Gotland and Arkona Basins have generally the highest degree of cylisation of their brGDGTs. (For interpretation of the references to colour in this figure legend, the reader is referred to the web version of this article.)

(e.g. 223 cm; see Fig. 10) is such that they still plot outside the global soil dataset.

We conclude that in the brackish period for both basins, the input of soil-derived brGDGTs was relatively minor and the majority of brGDGTs was produced in situ in the alkaline pore waters of the marine sediments, or perhaps, in the water column. However, at times of anoxic bottom water conditions, an additional unknown source of brGDGTs played a role in the brGDGT provenance.

5.1.2. The pre-brackish phases

The brGDGTs in the sediments deposited before the brackish period (i.e. during the Ancylus Lake, the Yoldia Sea, and the Ice Lake phases) reveal fundamental differences compared to those deposited in the brackish period. Firstly, the brGDGT concentration (normalised on TOC) increased by an order of magnitude or more. Since the crenarchaeol concentrations remained the same or declined, this resulted in a marked increase of the BIT index in both the Gotland (Fig. 3d) and Arkona (Figs. 4d and 9d) Basin at the transition to the brackish phase. In the GDGT ternary diagram (Fig. 5) all these pre-brackish phase sediments plot in the "non-marine" area, where sediments from lakes and soils are typically found (cf. Schouten et al., 2013). This indicates that these sedimentary brGDGTs are derived from aquatic production or from eroded soil material washed into the BS (mostly a lake at that time). A second prominent feature is that their distributions of the brackish and these earlier phases are remarkably different; penta- and hexamethylated brGDGTs are much more abundant (Fig. 10). The strong increase in the degree of methylation is also revealed by the MBT'_{5Me} that in the pre-brakish phases drops to values <0.2 for the Gotland and <0.3 for the Arkona Basin (Figs. 8c and 9c). All pre-brackish phase sediments have a brGDGT distribution different from those of soils (Fig. 10a) and more similar to that of low-temperature lakes (Fig. 10b). Hence, the transport of soil-derived brGDGTs is not an important source as they seem to be mostly derived from in situ aquatic production. Indeed, in situ production is thought to be a major brGDGT source in a variety of lake systems (e.g. Tierney and Russell, 2009; Sinninghe Damsté et al., 2009; Buckles et al., 2014; Weber et al., 2015).

A predominant aquatic brGDGT origin during these phases is supported by two other observations. Firstly, sedimentary brGDGT concentrations in various lake systems are substantially higher than in the soils of the lake watershed (Tierney and Russell, 2009; Loomis et al., 2011; Buckles et al., 2014; Tierney et al., 2012). The brGDGT concentrations in the pre-brackish phase are comparable or higher than those in lakes and substantially higher than in soils, making a predominant soil origin unlikely. Secondly, the presence of the novel hexamethylated brGDGT IIIa″ during most of the Ancylus Lake and Yoldia Sea phases in both basins (Figs. 8d and 9d) provides evidence for in situ production of at least some brGDGTs. IIIa″ was recently identified in sediments of an eutrophic Swiss mountain lake (Lake Hinterburg), where its absence from the watershed soils indicated that its source is exclusively lacustrine in situ production (Weber et al., 2015).

A further check for potential in situ production is the determination of the stable carbon isotope composition of the alkyl

moieties of brGDGTs ($\delta^{13}C_{brGDGT}$). In Lake Hinterburg $\delta^{13}C_{brGDGT}$ in the sediment (ca. −43‰) was found to be substantially lower than (i) $\delta^{13}C_{brGDGT}$ values measured in soils from the watershed (ca. −27‰), and (ii) the $\delta^{13}C$ of sedimentary TOC (−34‰) (Weber et al., 2015). This stark ^{13}C-depletion of brGDGTs was attributed to extensive microbial C recycling within the lake that led to ^{13}C depletion in the dissolved and particulate carbon pools, which in turn served as a carbon source for the aquatic brGDGT-producing microbes. Three intervals of the Gotland Basin sedimentary record from both the Ancylus Lake and Yoldia Sea phases with the highest fractional abundance of brGDGT IIIa″ were selected to determine if the majority of the brGDGTs from these periods were in fact produced in situ. However, in contrast to Lake Hinterburg, the presence of the in situ-produced brGDGT IIIa″ was not linked to such low $\delta^{13}C_{(brGDGT)}$ values in the BS sections analyzed (−27.4 to −29.0‰; Table 2), which were similar to $\delta^{13}C_{TOC}$ values measured in soils (−26 to −28‰; Table 2) and, therefore, could not further support an origin of brGDGTs from aquatic C pools.

Based on the fractional abundances of the tetra-, penta- and hexamethylated brGDGTs (Fig. 10), their high concentrations, and the presence of the novel IIIa″ brGDGT in the sedimentary record, we conclude that aquatic in situ production was the primary brGDGT source in the pre-brackish period sediments. This is not in contradiction with the high values of the BIT index in this interval (Figs. 8d and 9d). In lakes the BIT index is determined by the balance between production of crenarchaeol by ammonium-oxidizing Thaumarchaeota (Buckles et al., 2013) and in situ brGDGT production (Buckles et al., 2014, 2016) and is commonly quite high (e.g. Blaga et al., 2009; Tierney et al., 2010). Several maxima in the BIT index records are evident during the lower salinity phases (Figs. 8 and 9). Both BIT index maxima (at 305 and 375 cm composite depth; Fig. 3d) in the Gotland Basin are predominantly due to decreased crenarchaeol concentrations (Fig. 3b and c). In the Arkona basin a broad BIT index maximum, recording the highest values (i.e. 0.90), occurred in the middle part of the Ancylus Lake section (Fig. 9d). In contrast to the Gotland Basin record, both the concentration of brGDGTs and crenarchaeol increased during this maximum (Fig. 4b and c), suggesting perhaps a different mechanism, e.g. by an increase in terrigenous input. Peat may contain high brGDGT concentrations (Weijers et al., 2011). In order to determine if peat erosion may have been responsible for the BIT index maximum, four sediment horizons from around the maximum (Table 3) were analyzed for specific peat markers. Baas et al. (2000) showed that *Sphagnum*, an abundant species in peat bogs, is characterized by a dominance of the C_{23} or C_{25} *n*-alkanes. Our results showed that the C_{23} and C_{25} *n*-alkanes were abundant (average ratio of $C_{23} + C_{25}$ compared with total *n*-alkanes is 0.27 ± 0.04; Table 3), confirming a contribution of *Sphagnum* and thus peat to the Arkona Basin sediments during the Ancylus Lake phase. Kaiser and Arz (2016) also showed that *n*-alkane distributions of BS surface sediments indicated a contribution from peat in the northern and southern regions. However, since the ratio of $C_{23} + C_{25}$ relative to total *n*-alkanes did not substantially increase with increasing BIT index values, an increased influx of peat is unlikely to explain the higher BIT index values. Therefore, the variations in the BIT index are most likely explained by the balance of production of crenarchaeol and brGDGTs.

Quite substantial changes in the brGDGT distribution in the pre-brackish phase sediments are noted. For the Gotland Basin the MBT'_{5Me} remains stable (Fig. 8c) but for the Arkona Basin an increase towards values of 0.5 are noted at the Yoldia Sea – Ancylus Lake transition (Fig. 9c). The #rings and IR records show even more variation (Figs. 8 and 9) and may be related to changes in pH or in the brGDGT-producing microbial population. Interpretation of these changes will require more in-depth knowledge of lacustrine in situ brGDGT production. In any case, the brGDGT distribution in the Yoldia Sea phase of both basins is rather different from those in the brackish phase. This suggests that, although during both phases the BS was connected to the sea, the short duration of the connection in the Yoldia Sea phase did not result in conditions that were similar to those encountered during most of the brackish phase.

Table 3
BIT index values and ratio of ($C_{23} + C_{25}$)/total n-alkanes, demonstrating the dominance of *Sphagnum* plants indicating the presence of peat (Baas et al., 2000), for samples with BIT values above 0.7 from the Arkona Basin during the Ancylus Lake phase.

Sediment core	Sediment core depth (cm)	BIT index	($C_{23} + C_{25}$)/total n-alkanes
318340	540.5	0.69	0.25
318340	599.5	0.81	0.27
318340	634.5	0.82	0.23
318310	642.5	0.90	0.32

5.1.3. The Ancylus Lake – Littorina Sea transition

A detailed examination of the Ancylus Lake/Littorina Sea transition in the Gotland Basin, where this transition was studied in high resolution, reveals a number of stepwise changes. The largest changes are seen at ca. 250 cm composite depth where the BIT index drops substantially to a value <0.1 due to rapidly decreasing brGDGT concentrations (Fig. 3), the MBT'_{5Me} rapidly increased (Fig. 8c), and TOC content increased to the minimal levels observed in the brackish phase (Fig. 3a). This is where we, on the basis of the GDGT composition, place the boundary between the Ancylus Lake and Littorina Sea phase. However, it should be noted that based on the diatom record the Ancylus Lake/Littorina Sea boundary is placed at 230 cm composite depth (Moros, unpublished results), 20 cm higher up in the section, which corresponds to a time gap of ca. 200 years (Warden et al., 2017). From 250 cm upwards, MBT'_{5Me} increased further, ultimately reaching values of >0.5 at 242 cm, and these higher values characterized most of the brackish phase (Fig. 8c). At the same time, #rings increased reaching values >0.8 at 241–243 cm for a short period, the highest values observed throughout the brackish phase (Fig. 8a). The sediments above this interval were sampled in lower resolution, but reveal a strong drop in #rings to the lowest value of the brackish phase at 225 cm (0.29), where the sediments are laminated and have the highest TOC content of the brackish phase. At 227 cm (i.e. just before the minimum in #rings), a sudden drop in MBT'_{5Me} and IR (Fig. 8) and an increase in the BIT index and brGDGT concentration (Fig. 3) is observed.

The discrepancy in the boundary between the Ancylus Lake and Littorina Sea phases likely relates to the fact that the changes in diatom assemblages record the changes in surface salinity, which changed from fresh to brackish, whilst the brGDGTs predominantly record changes in the deeper waters. The connection with the North Sea resulted in the inflow of salt water and because salt water is more dense, this influx probably first affected the Gotland Basin bottom waters. This increase in salinity led to impoverished conditions for brGDGT-producing microbes in the Ancylus Lake deep water, resulting in a substantial decrease in brGDGT concentration. Subsequently, the salinity of the bottom waters increased further to such an extent that brGDGT-producing microbes found a niche in the surface sediments, just like during the LIA, which is evident from the distinct peak in #rings (Fig. 8c). As the Gotland Basin became strongly stratified, the organic matter preservation due to anoxic bottom waters increased, however, this probably had a strong effect on the benthic and, probably oxygen-requiring brGDGT-producing microbes. When the incursion of North Sea waters also affected the salinity of the Gotland Basin

photic zone, this resulted in a marked change in the diatom composition. Hence, the transition from the Ancylus Lake to the Littorina Sea was likely gradual, first affecting the salinity of the bottom waters and then later that of the surface waters.

5.2. Potential palaeoclimate application of brGDGTs

The heterogeneity of brGDGT sources in the BS basin greatly complicates the use of brGDGTs as a temperature proxy. Some recent developments, however, allow us to explore some new approaches.

A Bothnian Sea sediment (377850) had the highest BIT index (0.31) and the lowest #rings value of all surface sediments, indicating that this site received the highest soil-derived brGDGT contribution. This is remarkable since other sampling sites (i.e. 372820, 377830, and 349200) were closer to the mouth of a river, thought to be a predominant continental brGDGTs source (e.g. Zell et al., 2013), However, these sediments did not have correspondingly higher BIT index values (Table 1; Fig. 2). Perhaps the Bothnian Sea site received more terrestrial material or in situ production was low in this area and hence the terrestrial signal was not overwhelmed by in situ produced brGDGTs. We applied the soil calibration based on individually quantified 5- and 6-methyl brGDGTs from De Jonge et al. (2014a) to reconstruct continental pH and MAT. The CBT′-derived reconstructed pH (see Eqs. (10) and (11)) was 6.4, which is close to the reported average of soils in the Baltic region (6.1; Reimann et al., 2000). The reconstructed temperature using the MBT'_{5Me} calibration (12) is 4.3 °C, similar to the measured MAT of 4.5 °C from the closest weather station (Table 1). Apparently, the cold winters in this region, which may limit microbial production in soil, do not result in a bias of MBT'_{5Me}-derived temperatures. Consequently, the Bothnian Sea may be a good location for collecting sediment cores for future brGDGT-based continental climate reconstructions in the BS area.

A soil calibration is, however, not suitable for the other surface sediments since the brGDGTs are predominantly derived from in situ production. Recently, a novel MBT'_{5Me} calibration for calculating bottom water temperatures (BWT) (Dearing Crampton Flood et al., 2018) was developed for coastal marine sediments where brGDGTs are predominantly in situ produced. Predicted BWT for BS surface sediments varied substantially ranging from −1.2 to 9.0 °C with a clear trend toward higher temperatures at lower latitudes. Measured MATs from weather stations close to these sites ranged from 1.4 to 8.1 °C (Table 1). The positive correlation of the estimated BWTs and the MATs from the closest weather stations was significant, $R^2 = 0.82$ ($n = 11$), providing confidence in this new calibration. Estimated BWTs were 6–9 and 9 °C for the Gotland and Bornholm basins, respectively, which is in fairly good agreement with their measured BWT over the last 20 years of 5–6 °C and 6.5–8.0 °C, respectively (Carstensen et al., 2014). The offsets in the BWT estimates are likely due to the fact that the sedimentary brGDGTs are not purely derived from in situ production but also from soil erosion. However, since the MBT'_{5Me}-based temperature calibrations for sedimentary in situ production and soils are quite similar (Dearing Crampton Flood et al., 2018), the offsets due to mixing may be limited in cold areas such as the BS. However, the estimated average BWT for the Skagerrak surface sediments, 17 °C, was unrealistically high. Earlier brGDGT-derived MAT from Skagerrak sediments using a soil calibration (Rueda et al., 2009) were also high (15.5 °C). It was postulated that this could be due to brGDGT transport from the southern North Sea or alternatively that in this region the organisms that produced the brGDGTs were more active during the summer since Scandinavian soils are mostly snow covered during the winter months.

Because in situ production was an important brGDGT source during the brackish phase, the new marine coastal BWT calibration (Dearing Crampton Flood et al., 2018) was applied. However, this had to be limited to sedimentary brGDGTs with a predominantly aquatic origin and, therefore, this was only performed for sediments with #rings >0.7. For the Arkona Basin, BWT could be calculated for all but one of the brackish phase sediments, resulting in an estimate of 9.2 ± 1.6 °C. For the Gotland Basin only a limited number of sediments have a #rings >0.7 (Fig. 8a). Sediments for the LIA (11.5–29 cm) have an estimated BWT of 6.3 ± 1.1 °C, which is slightly higher than reported BWTs of ca. 4 °C for the period 1890–1930 (Carstensen et al., 2014). Just below the MCA (at 70 and 100 cm composite depth) there are two sediments for which BWT can be estimated to be 5–6 °C. Since the Arkona Basin is more shallow and is more to the south, it makes sense that this BWT estimate (9.2 ± 1.6 °C) is higher than for the Gotland Basin. The other section for which BWT in the Gotland Basin can be estimated is when the connection with the North Sea had just been established and a peak in #rings is observed (see Section 5.1.3; Fig. 8a); estimated BWT is here ca. 7 °C. Hence, it seems that during the brackish phase when the BIT index was low and #rings was high, the marine coastal sediment calibration performed well for reconstructing BWT.

For the Ancylus Lake, Yoldia Sea and Ice Lake phases aquatic in situ production in a large lake setting seems to be the dominant source for brGDGTs. Hence, if we want to reconstruct temperatures using these brGDGTs, we will have to apply a lacustrine calibration. A number of calibrations have been developed to this end, including the global lake calibration developed by Pearson et al. (2011). However, all of these calibrations are based on calibration sets that have been obtained using chromatographic methods that result in an inadequate separation of the 5- and 6-methyl brGDGTs. It has been demonstrated that separation of these isomers results in substantially improved calibrations (e.g. De Jonge et al., 2014a, 2014b) and, therefore, should be applied. Recently, a regional lake calibration set has become available (Russell et al., 2018), which is based on 65 lakes in tropical East Africa from a variety of altitudes and, therefore, spanning a wide temperature range (2–27 °C). Before applying this calibration to the Baltic data set, brGDGT distributions of the different datasets were compared (Fig. 10b). This shows that the African lake datapoints plot in a restricted area just as is the case for soils (Fig. 10a; cf. Sinninghe Damsté, 2016), with the higher temperature lakes plotting to the right and low temperature lakes towards the lefthand corner. The comparison also reveals that some but not all BS pre-brackish phase datapoints follow the trend of the African lake sediments (Fig. 10b). The Gotland Basin sediments of the Ancylus Lake and Yoldia Sea phases plot in close vicinity of the coldest African lakes. The MBT'_{5Me} is quite constant in these phases (Fig. 8c) and application of the lake calibration results in mean temperatures of 3 ± 1 and 4 ± 1 °C for the Ancylus Lake and Yoldia Sea phases, respectively. For the Arkona Basin this exercise is less straightforward since many data points do not plot in the vicinity of the African lake dataset (Fig. 10c); they are characterized by a higher fractional abundance of tetramethylated (approaching 45% for some Ancylus Lake phase sediments) and a lower fractional abundance of pentamethylated brGDGTs. These sediments roughly correspond to the 600–840 cm section, where MBT'_{5Me} increases to values of 0.5, which would correspond to unrealistically high temperatures of ca. 15 °C (Fig. 9c). When only Ancylus Lake phase sediments with a fractional abundance of tetramethylated brGDGTs <20% (i.e. where they overlap the area of the African lake data points in the ternary diagram; Fig. 10b) are taken into consideration, temperature estimates are 8 ± 2 °C, which is higher than for the Gotland Basin. The brGDGT distributions of the Yoldia Sea and Ice Lake phases (Fig. 10b) reveal that most of them do not qualify for calculation of temperatures using the African Lake calibration.

These data indicate that it remains rather complicated to extract palaeotemperature data from the BS brGDGT record. Under certain circumstances, we can extract BWT during the brackish phase and temperature information during the lake phases. However, more knowledge is required, especially on brGDGT production in temperate lakes, before these data can be interpreted with full confidence. At sites where brGDGT sources have been constant through time brGDGTs remain a useful tool for paleotemperature reconstruction.

6. Conclusions

Marked changes in brGDGT distribution and the BIT index occurred concomitantly with the re-establishment of the connection between the BS and the North Sea. These shifts were likely caused by the change in the brGDGT sources from water column in situ production during the lower salinity phases to in situ production by benthic microbes during the brackish phase. The contribution of continental brGDGTs to Holocene BS sediments through erosion of soil seems in general not to be substantial. In situ brGDGT production over the Holocene confound their use for continental temperature reconstructions in the BS. After thorough assessment of brGDGT provenance, however, temperature estimates can still be meaningful if appropriate calibrations are applied. Our results further indicate that changes in brGDGT distribution, in turn, can be used to reconstruct past environmental changes such as freshening and saltening of a basin. Hence, factors controlling sedimentary brGDGT composition should be further investigated using suitable sedimentary records from other regions spanning known environmental changes to further explore this exciting possibility.

Acknowledgements

We thank two anonymous referees and the associate editor for their comments, J. Ossebaar and E.C. Hopmans for their help with the UHPLC-APCI-MS analysis, and A. Mets and M. Sollai for help with sample preparation. This research was supported by funding from the European Research Council under the European Union's Seventh Framework Programme (FP7/2007-2013)/ERC grant agreement n° [226600]. JSSD also receives funding from the Netherlands Earth System Science Center (NESSC) though a gravitation grant (024.002.001) from the Dutch Ministry for Education, Culture and Science.

Associate Editor—**Stuart Wakeham**

References

Andrén, E., Andrén, T., Kunzendorf, H., 2000a. Holocene history of the Baltic Sea as a background for assessing records of human impact in the sediments of the Gotland Basin. Holocene 10, 687–702.

Andrén, E., Andrén, T., Sohlenius, G., 2000b. The Holocene history of the southwestern Baltic Sea as reflected in a sediment core from the Bornholm Basin. Boreas 29, 233–250.

Baas, M., Pancost, R., van Geel, B., Sinninghe Damsté, J.S., 2000. A comparative study of lipids in *Sphagnum* species. Organic Geochemistry 31, 535–541.

Bendle, J.A., Weijers, J.W., Maslin, M.A., Sinninghe Damsté, J.S., Schouten, S., Hopmans, E.C., Boot, C.S., Pancost, R.D., 2010. Major changes in glacial and Holocene terrestrial temperatures and sources of organic carbon recorded in the Amazon fan by tetraether lipids. Geochemistry Geophysics Geosystems 11, 12.

Berg, C., Listmann, L., Vandieken, V., Vogts, A., Jürgens, K., 2015. Chemoautotrophic growth of ammonia-oxidizing Thaumarchaeota enriched from a pelagic redox gradient in the Baltic Sea. Frontiers in Microbiology 5, 786.

Bianchi, T.S., Rolff, C., Lambert, C.D., 1997. Sources and composition of particulate organic carbon in the Baltic Sea: the use of plant pigments and lignin-phenols as biomarkers. Marine Ecology Progress Series 156, 25–31.

Björck, S., 1995. A review of the history of the Baltic Sea, 13.0–8.0 ka BP. Quaternary International 27, 19–40.

Björck, S., Kromer, B., Johnsen, S., Bennike, O., Hammarlund, D., Lemdahl, G., Possnert, G., Rasmussen, T.L., Wohlfarth, B., Hammer, C.U., Spurk, M., 1996. Synchronized terrestrial atmospheric deglacial records around the North Atlantic. Science 274, 1155–1160.

Blaga, C.I., Reichart, G.-J., Heiri, O., Sinninghe Damsté, J.S., 2009. Tetraether membrane lipid distributions in water-column particulate matter and sediments: a study of 47 European lakes along a north-south transect. Journal of Paleolimnolology 41, 523–540.

Buckles, L.K., Villanueva, L., Weijers, J.W.H., Verschuren, D., Sinninghe Damsté, J.S., 2013. Linking isoprenoidal GDGT membrane-lipid distributions with gene abundances of ammonia-oxidising Thaumarchaeota and an uncultured crenarchaeotal groups in the water column of a tropical lake (Lake Challa, East Africa). Environmental Microbiology 15, 2445–2462.

Buckles, L.K., Weijers, J.W., Verschuren, D., Sinninghe Damsté, J.S., 2014. Sources of core and intact branched tetraether membrane lipids in the lacustrine environment: anatomy of Lake Challa and its catchment, equatorial East Africa. Geochimica et Cosmochimica Acta 140, 106–126.

Buckles, L.K., Verschuren, D., Weijers, J.W.H., Cocquyt, C., Blaauw, M., Sinninghe Damsté, J.S., 2016. Interannual and (multi-)decadal variability in the sedimentary BIT index of Lake Challa, East Africa, over the past 2200 years: assessment of the precipitation proxy. Climate of the Past 12, 1243–1262.

Carstensen, J., Andersen, J.H., Gustafsson, B.G., Conley, D.J., 2014. Deoxygenation of the Baltic Sea during the last century. Proceedings of the National Academy of Sciences of the United States of America 11, 5628–5633.

Coolen, M.J., Abbas, B., van Bleijswijk, J., Hopmans, E.C., Kuypers, M.M., Wakeham, S. G., Sinninghe Damsté, J.S., 2007. Putative ammonia-oxidizing Crenarchaeota in suboxic waters of the Black Sea: a basin-wide ecological study using 16S ribosomal and functional genes and membrane lipids. Environmental Microbiology 9, 1001–1016.

Dean Jr, W.E., 1974. Determination of carbonate and organic matter in calcareous sediments and sedimentary rocks by loss on ignition: comparison with other methods. Journal of Sedimentary Research 44, 242–248.

Dearing Crampton Flood, E., Peterse, F., Munsterman, D., Sinninghe Damsté, J.S., 2018. Extracting Pliocene continental air temperature evolution in NW Europe from tetraether lipids archived in North Sea Basin sediments. Earth and Planetary Science Letters 490, 193–205.

De Jonge, C., Hopmans, E.C., Stadnitskaia, A., Rijpstra, W.I.C., Hofland, R., Tegelaar, E., Sinninghe Damsté, J.S., 2013. Identification of novel penta-and hexamethylated branched glycerol dialkyl glycerol tetraethers in peat using HPLC–MS^2, GC–MS and GC–SMB-MS. Organic Geochemistry 54, 78–82.

De Jonge, C., Hopmans, E.C., Zell, C.I., Kim, J.-H., Schouten, S., Sinninghe Damsté, J.S., 2014a. Occurrence and abundance of 6-methyl branched glycerol dialkyl glycerol tetraethers in soils: implications for palaeoclimate reconstruction. Geochimica et Cosmochimica Acta 141, 97–112.

De Jonge, C., Stadnitskaia, A., Hopmans, E.C., Cherkashov, G., Fedotov, A., Sinninghe Damsté, J.S., 2014b. In situ produced branched glycerol dialkyl glycerol tetraethers in suspended particulate matter from the Yenisei River, Eastern Siberia. Geochimica et Cosmochimica Acta 125, 476–491.

De Jonge, C., Stadnitskaia, A., Hopmans, E.C., Cherkashov, G., Fedotov, A., Streletskaya, I.D., Vasiliev, A.A., Sinninghe Damsté, J.S., 2015a. Drastic changes in the distribution of branched tetraether lipids in suspended matter and sediments from the Yenisei River and Kara Sea (Siberia): implications for the use of brGDGT-based proxies in coastal marine sediments. Geochimica et Cosmochimica Acta 165, 200–225.

De Jonge, C., Stadnitskaia, A., Fedotov, A., Sinninghe Damsté, J.S., 2015b. Impact of riverine suspended particulate matter on the branched glycerol dialkyl glycerol tetraether composition of lakes: the outflow of the Selenga River in Lake Baikal (Russia). Organic Geochemistry 83, 241–252.

De Jonge, C., Stadnitskaia, A., Cherkashov, G., Sinninghe Damsté, J.S., 2016. Branched glycerol dialkyl glycerol tetraethers and crenarchaeol record post-glacial sea level rise and shift in source of terrigenous brGDGTs in the Kara Sea (Arctic Ocean). Organic Geochemistry 92, 42–54.

Ding, S., Schwab, V.F., Ueberschaar, N., Roth, V.N., Lange, M., Xu, Y., Gleixner, G., Pohnert, G., 2016. Identification of novel 7-methyl and cyclopentanyl branched glycerol dialkyl glycerol tetraethers in lake sediments. Organic Geochemistry 102, 52–58.

Emeis, K.-C., Struck, U., Blanz, T., Kohly, A., Voβ, M., 2003. Salinity changes in the central Baltic Sea (NW Europe) over the last 10000 years. The Holocene 13, 411–421.

Hopmans, E.C., Weijers, J.W., Schefuß, E., Herfort, L., Sinninghe Damsté, J.S., Schouten, S., 2004. A novel proxy for terrestrial organic matter in sediments based on branched and isoprenoid tetraether lipids. Earth and Planetary Science Letters 224 (107–116), 2004.

Hopmans, E.C., Schouten, S., Sinninghe Damsté, J.S., 2016. The effect of improved chromatography on GDGT-based palaeoproxies. Organic Geochemistry 93 (1–6), 2016.

Huguet, C., Hopmans, E.C., Febo-Ayala, W., Thompson, D.H., Sinninghe Damsté, J.S., Schouten, S., 2006. An improved method to determine the absolute abundance of glycerol dibiphytanyl glycerol tetraether lipids. Organic Geochemistry 37, 1036–1041.

Jensen, J.B., 1995. A Baltic Ice Lake transgression in the southwestern Baltic: evidence from Fakse Bugt, Denmark. Quaternary International 27, 59–68.

Jensen, J.B., Bennike, O., Witkowski, A., Lemke, W., Kuijpers, A., 1999. Early Holocene history of the southwestern Baltic Sea: the Ancylus Lake stage. Boreas 28, 437–453.

Kabel, K., Moros, M., Porsche, C., Neumann, T., Adolphi, F., Andersen, T.J., Siegel, H., Gerth, M., Leipe, T., Jansen, E., Sinninghe Damsté, J.S., 2012. Impact of climate change on the Baltic Sea ecosystem over the past 1,000 years. Nature Climate Change 2, 871–874.

Kaiser, J., Arz, H.W., 2016. Sources of sedimentary biomarkers and proxies with potential paleoenvironmental significance for the Baltic Sea. Continental and Shelf Research 122 (102–119), 2016.

Kaneko, M., Kitajima, F., Naraoka, H., 2011. Stable hydrogen isotope measurement of archaeal ether-bound hydrocarbons. Organic Geochemistry 42, 166–172.

Loomis, S.E., Russell, J.M., Sinninghe Damsté, J.S., 2011. Distributions of branched GDGTs in soils and lake sediments from western Uganda: implications for a lacustrine paleothermometer. Organic Geochemistry 42, 739–751.

Loomis, S.E., Russell, J.M., Ladd, B., Street-Perrott, F.A., Sinninghe Damsté, J.S., 2012. Calibration and application of the branched GDGT temperature proxy on East African lake sediments. Earth and Planetary Science Letters 357, 277–288.

Naafs, B.D.A., Inglis, G.N., Zheng, Y., Amesbury, M.J., Biester, H., Bindler, R., Blewett, J., Burrows, M.A., del Castillo Torres, D., Chambers, F.M., Cohen, A.D., Evershed, R.P., Feakins, S.J., Gałka, M., Gallego-Sala, A., Gandois, L., Gray, D.M., Hatcher, P. G., Honorio Coronado, E.N., Hughes, P.D.M., Huguet, A., Könönen, M., Laggoun-Défarge, F., Lähteenoja, O., Lamentowicz, M., Marchant, R., McClymont, E., Pontevedra-Pombal, X., Ponton, C., Pourmand, A., Rizzuti, A.M., Rochefort, L., Schellekens, J., De Vleeschouwer, F., Pancost, R.D., 2017. Introducing global peat-specific temperature and pH calibrations based on brGDGT bacterial lipids. Geochimica et Cosmochimica Acta 208, 285–301.

Niemann, H., Stadnitskaia, A., Wirth, S.B., Gilli, A., Anselmetti, F.S., Sinninghe Damsté, J.S., Schouten, S., Hopmans, E.C., Lehmann, M.F., 2012. Bacterial GDGTs in Holocene sediments and catchment soils of a high Alpine lake: application of the MBT/CBT-paleothermometer. Climate of the Past 8, 889–906.

Pearson, E.J., Juggins, S., Talbot, H.M., Weckstrom, J., Rosen, P., Ryves, D.B., Roberts, S. J., Schmidt, R., 2011. A lacustrine GDGT-temperature calibration from the Scandinavian Arctic to Antarctic: renewed potential for the application of GDGT-paleothermometry in lakes. Geochimica et Cosmochimica Acta 75, 6225–6238.

Peterse, F., Kim, J.-H., Schouten, S., Kristensen, D.K., Koç, N., Sinninghe Damsté, J.S., 2009. Constraints on the application of the MBT/CBT palaeothermometer at high latitude environments (Svalbard, Norway). Organic Geochemistry 40, 692–699.

Peterse, F., Nicol, G.W., Schouten, S., Sinninghe Damsté, J.S., 2010. Influence of soil pH on the abundance and distribution of core and intact polar lipid-derived branched GDGTs in soil. Organic Geochemistry 41, 1171–1175.

Peterse, F., Prins, M.A., Beets, C.J., Troelstra, S.R., Zheng, H., Gu, Z., Schouten, S., Sinninghe Damsté, J.S., 2011. Decoupled warming and monsoon precipitation in East Asia over the last deglaciation. Earth and Planetary Science Letters 301, 256–264.

Punning, J., Martma, T., Kessel, H., Vaikme, R., 1988. The isotopic composition of oxygen and carbon in the subfossil mollusc shells of the Baltic Sea as an indicator of palaeosalinity. Boreas 17, 27–31.

Reimann, C., Siewers, U., Tarvainen, T., Bityukova, L., Eriksson, J., Gilucis, A., Gregorauskiene, V., Lukashev, V., Matinian, N.N., Pasieczna, A., 2000. Baltic soil survey: total concentrations of major and selected trace elements in arable soils from 10 countries around the Baltic Sea. Science of the Total Environment 257, 155–170.

Rueda, G., Rosell-Mele, A., Escala, M., Gyllencreutz, R., Backman, J., 2009. Comparison of instrumental and GDGT-based estimates of sea surface and air temperatures from the Skagerrak. Organic Geochemistry 40, 287–291.

Russell, J.M., Hopmans, E.C., Loomis, S.E., Liang, J., Sinninghe Damsté, J.S., 2018. Distributions of 5- and 6-methyl branched glycerol dialkyl glycerol tetraethers (brGDGTs) in East African lake sediment: effects of temperature, pH, and new lacustrine paleotemperature calibrations. Organic Geochemistry 117, 56–69.

Schouten, S., Hoefs, M.J.L., Koopmans, M.P., Bosch, H.-J., Sinninghe Damsté, J.S., 1998. Structural characterization, occurrence and fate of archaeal ether-bound acyclic and cyclic biphytanes and corresponding diols in sediments. Organic Geochemistry 29, 1305–1319.

Schouten, S., Hopmans, E.C., Sinninghe Damsté, J.S., 2013. The organic geochemistry of glycerol dialkyl glycerol tetraether lipids: a review. Organic Geochemistry 54, 19–61.

Sinninghe Damsté, J.S., Hopmans, E.C., Pancost, R.D., Schouten, S., Geenevasen, J.A.J., 2000. Newly discovered non-isoprenoid glycerol dialkyl glycerol tetraether lipids in sediments. Chemical Communications 17, 1683–1684.

Sinninghe Damsté, J.S., Schouten, S., Hopmans, E.C., van Duin, A.C., Geenevasen, J.A. J., 2002. Crenarchaeol the characteristic core glycerol dibiphytanyl glycerol tetraether membrane lipid of cosmopolitan pelagic crenarchaeota. Journal of Lipid Research 43, 1641–1651.

Sinninghe Damsté, J.S., Ossebaar, J., Abbas, B., Schouten, S., Verschuren, D., 2009. Fluxes and distribution of tetraether lipids in an equatorial African lake: constraints on the application of the TEX_{86} palaeothermometer and BIT index in lacustrine settings. Geochimica et Cosmochimica Acta 73, 4232–4249.

Sinninghe Damsté, J.S., 2016. Spatial heterogeneity of sources of branched tetraethers in shelf systems: the geochemistry of tetraethers in the Berau River delta (Kalimantan, Indonesia). Geochimica et Cosmochimica Acta 186, 13–31.

Sollai, M., Hopmans, E.C., Bale, N.J., Mets, A., Warden, L., Moros, M., Sinninghe Damsté, J.S., 2017. The Holocene sedimentary record of cyanobacterial glycolipids in the Baltic Sea: evaluation of their application as tracers of past nitrogen fixation. Biogeosciences 4, 5789–5804.

Sternbeck, J., Sohlenius, G., 1997. Authigenic sulfide and carbonate mineral formation in Holocene sediments of the Baltic Sea. Chemical Geology 135, 55–73.

Suess, E., 1979. Mineral phases formed in anoxic sediments by microbial decomposition of organic matter. Geochimica et Cosmochimica Acta 43, 339–352.

Tierney, J.E., Russell, J.M., 2009. Distributions of branched GDGTs in a tropical lake system: implications for lacustrine application of the MBT/CBT paleoproxy. Organic Geochemistry 40, 1032–1036.

Tierney, J.E., Russell, J.M., Eggermont, H., Hopmans, E.C., Verschuren, D., Sinninghe Damsté, J.S., 2010. Environmental controls on branched tetraether lipid distributions in tropical East African lake sediments. Geochimica et Cosmochimica Acta 74, 4902–4918.

Tierney, J.E., Schouten, S., Pitcher, A., Hopmans, E.C., Sinninghe Damsté, J.S., 2012. Core and intact polar glycerol dialkyl glycerol tetraethers (GDGTs) in Sand Pond, Warwick, Rhode Island (USA): insights into the origin of lacustrine GDGTs. Geochimica et Cosmochimica Acta 77, 561–581.

Tikkanen, M., Oksanen, J., 2002. Late Weichselian and Holocene shore displacement history of the Baltic Sea in Finland. Fennia International Journal of Geography 180, 9–20.

Warden, L., van der Meer, M., Moros, M., Sinninghe Damsté, J.S., 2016a. Sedimentary alkenone distributions reflect salinity changes in the Baltic Sea over the Holocene. Organic Geochemistry 102, 30–44.

Warden, L., Kim, J.-H., Zell, C., Vis, G.-J., de Stitger, H., Bonnin, J., Sinninghe Damsté, J. S., 2016b. Examining the provenance of branched GDGTs in the Tagus River drainage basin and it outflow into the Atlantic Ocean over the Holocene to determine their usefulness for paleoclimate applications. Biogeosciences 13, 5719–5738.

Warden, L., Moros, M., Neumann, T., Shennan, S., Timpson, A., Manning, K., Sollai, M., Wacker, L., Perner, K., Häusler, K., Leipe, T., Zillén, L., Kotilainen, A., Jansen, E., Schneider, R.R., Oeberst, R., Arz, H., Sinninghe, Damsté J.S., 2017. Climate induced human demographic and cultural change in northern Europe during the mid-Holocene. Scientific Reports 7, 15251.

Wasmund, N., 1997. Occurrence of cyanobacterial blooms in the Baltic Sea in relation to environmental conditions. International Review of Hydrobiology 82, 169–184.

Weber, Y., De Jonge, C., Rijpstra, W.I.C., Hopmans, E.C., Stadnitskaia, A., Schubert, C.J., Lehmann, M.F., Sinninghe Damsté, J.S., Niemann, H., 2015. Identification and carbon isotope composition of a novel branched GDGT isomer in lake sediments: evidence for lacustrine branched GDGT production. Geochimica et Cosmochimica Acta 154, 118–129. 2015.

Weijers, J.W.H., Schouten, S., Hopmans, E.C., Geenevasen, J.A.J., David, O.R.P., Coleman, J., Pancost, R.D., Sinninghe Damsté, J.S., 2006a. Membrane lipids of mesophilic anaerobic bacteria thriving in peats have typical archaeal traits. Environmental Microbiology 8, 648–657.

Weijers, J.W.H., Schouten, S., Spaargaren, O.C., Sinninghe Damsté, J.S., 2006b. Occurrence and distribution of tetraether membrane lipids in soils: implications for the use of the TEX_{86} proxy and the BIT index. Organic Geochemistry 37, 1680–1693.

Weijers, J.W.H., Schouten, S., van den Donker, J.C., Hopmans, E.C., Sinninghe Damsté, J.S., 2007a. Environmental controls on bacterial tetraether membrane lipid distribution in soils. Geochimica et Cosmochimica Acta 71, 703–713.

Weijers, J.W.H., Schefuß, E., Schouten, S., Sinninghe Damsté, J.S., 2007b. Coupled thermal and hydrological evolution of tropical Africa over the last deglaciation. Science 315, 1701–1704.

Weijers, J.W.H., Wiesenberg, G.L.B., Bol, R., Hopmans, E.C., Pancost, R.D., 2010. Carbon isotopic composition of branched tetraether membrane lipids in soils suggest a rapid turnover and a heterotrophic life style of their source organism (s). Biogeosciences 7, 2959–2973.

Weijers, J.W.H., Steinmann, P., Hopmans, E.C., Schouten, S., Sinninghe Damsté, J.S., 2011. Bacterial tetraether membrane lipids in peat and coal. Testing the MBT-CBT temperature proxy for climate reconstruction. Organic Geochemistry 42, 477–486.

Weijers, J.W.H., Schefuß, E., Kim, J.H., Sinninghe Damsté, J.S., Schouten, S., 2014. Constraints on the sources of branched tetraether membrane lipids in distal marine sediments. Organic Geochemistry 72, 14–22.

Winterhalter, B., 1992. Late-Quaternary stratigraphy of Baltic Sea basins – a review. Bulletin of the Geological Society of Finland 64, 189–194.

Yang, G., Zhang, C.L., Xie, S., Chen, Z., Gao, M., Ge, Z., Yang, Z., 2013. Microbial glycerol dialkyl glycerol tetraethers from river water and soil near the Three Gorges Dam on the Yangtze River. Organic Geochemistry 56, 40–50.

Zech, R., Gao, L., Tarozo, R., Huang, Y., 2012. Branched glycerol dialkyl glycerol tetraethers in Pleistocene loess-paleosol sequences: three case studies. Organic Geochemistry 53, 38–44.

Zell, C., Kim, J.H., Moreira-Turcq, P., Abril, G., Hopmans, E.C., Bonnet, M.P., Sobrinho, R.L., Sinninghe Damsté, J.S., 2013. Disentangling the origins of branched tetraether lipids and crenarchaeol in the lower Amazon River: implications for GDGT-based proxies. Limnology and Oceanography 58, 343–353.

Zell, C., Kim, J.-H., Hollander, D., Lorenzoni, L., Baker, P., Silva, C., Nittrouer, C., Sinninghe Damsté, J.S., 2014. Sources and distribution of branched and isoprenoid tetraether lipids on the Amazon shelf and fan: implications for the

use of GDGT-based paleothermometers in marine sediments. Geochimica et Cosmochimica Acta 139, 293–312.
Zhu, C., Weijers, J.W., Wagner, T., Pan, J.M., Chen, J.F., Pancost, R.D., 2011. Sources and distributions of tetraether lipids in surface sediments across a large river-dominated continental margin. Organic Geochemistry 42, 376–386.
Zink, K.G., Vandergoes, M.J., Mangelsdorf, K., Dieffenbacher-Krall, A.C., Schwark, L., 2010. Application of bacterial glycerol dialkyl glycerol tetraethers (GDGTs) to develop modern and past temperature estimates from New Zealand lakes. Organic Geochemistry 41, 1060–1066.